12-14-2018

Transcriptome-Wide Analysis of VSV Strains with Varying Ability to Block NF-κB

Thomas M. Russell
tmr8387@rit.edu

Transcriptome-Wide Analysis of VSV Strains with Varying Ability to Block NF-κB

by

Thomas M. Russell

A Thesis Submitted in Partial Fulfillment of the Requirements for the Degree of Master of Science in Bioinformatics

Thomas H. Gosnell School of Life Sciences
College of Science

Rochester Institute of Technology
Rochester, NY

December 14, 2018

Rochester Institute of Technology
Thomas H. Gosnell School of Life Sciences
Bioinformatics Program

To: Head, Thomas H. Gosnell School of Life Sciences

The undersigned state that Thomas Russell, a candidate for the Master of Science degree in Bioinformatics, has submitted his thesis and has satisfactorily defended it.

This completes the requirements for the Master of Science degree in Bioinformatics at Rochester Institute of Technology.

Thesis committee members:

Name	**Date**
Maureen C. Ferran, Ph.D. Thesis Advisor	
Feng Cui, Ph.D.	
Matthew Morris, Ph.D.	
Julie A. Thomas, Ph.D.	

Abstract

Vesicular stomatitis virus (VSV) is a negative sense, single-stranded RNA (ssRNA) virus that is currently studied for its uses as a vaccine viral vector and its potential in oncolytic therapy. The M protein of VSV is the active participant in the virus's abrogation of the host innate immune response. This activity is thought to be due to the M protein's ability to downregulate overall host transcription by blocking nuclear transport. A VSV mutant containing a D52G mutation in the M protein (22-20) has been shown to block nuclear transport while being defective as a suppressor of NF-κB activation. It is thus believed that while previous M protein mutant viruses are defective in both host transcription suppression and NF-κB activation, 22-20 is deficient in only one of these activities. This study aims to identify differentially expressed genes (DEGs) and pathways through transcriptome analysis of host response to VSV mutants. Our research leads us to believe that 22-20 does in fact down regulate overall host transcription, while being inefficient in suppressing NF-κB mediated immune response pathways. We also discovered important DEGs in the apoptosis pathway, including the antiapoptotic protein Mcl1, where downregulated by 22-20 to a greater degree than another mutant, 22-25. This combination of factors, deficiency in NF-κB suppression and increased apoptotic activation, could make 22-20 an interesting candidate for oncolytic research.

TABLE OF CONTENTS

Abbreviations and Acronyms

Introduction

Introduction to the Virus

Vesicular stomatitis virus (VSV) is the prototypical member of the family Rhabdoviridae. Unlike many viruses, VSV can infect a diverse number of vertebrate and invertebrate hosts, and even some species of plants. Although the virus has a broad host range, its preferred hosts include horses, mules, cattle, bison, sheep, goats, and pigs. Clinical signs of infection include the formation of vesicles, on the skin on the muzzle, tongue, teats and above the hooves of susceptible livestock. Although VSV typically causes a non-fatal infection in mammals, it creates a burdensome socio-economic issue when it infects these livestock. In contrast to rabies, a closely related virus that is also a member of the Rhabdovirus family, VSV rarely infects humans outside of select cases, and only causes self-limiting, flu-like symptoms (3).

Like other members of the Rhabdoviridae family, the VSV particle is bullet shaped (Figure 1) and is composed of two main components: the nucleocapsid or ribonuleoprotein (RNP) core group and the envelope group (3). Each component has specialized functions. The nucleoprotein (N) encapsidates the viral RNA, thus forming the RNP core. This binding protects the genome from degradation once inside the host cell. The matrix (M) protein is a bridging molecule between the central RNP and the plasma membrane. It is also responsible for several other functions including regulation of apoptosis and inhibition of host RNA polymerase II and III activity. The transmembrane glycoprotein (G) protein is essential for attachment of the virus to the cellular receptor. Together, the catalytic large (L) protein and the non-catalytic phosphoprotein (P) form the viral RNA-dependent RNA polymerase complex which drives the

production of new viral RNA during replication and transcription. This complex adds a poly A tail to one end of each viral mRNA and also adds a modified cap structure to the other end, which enables its recognition by the host ribosomes (3).

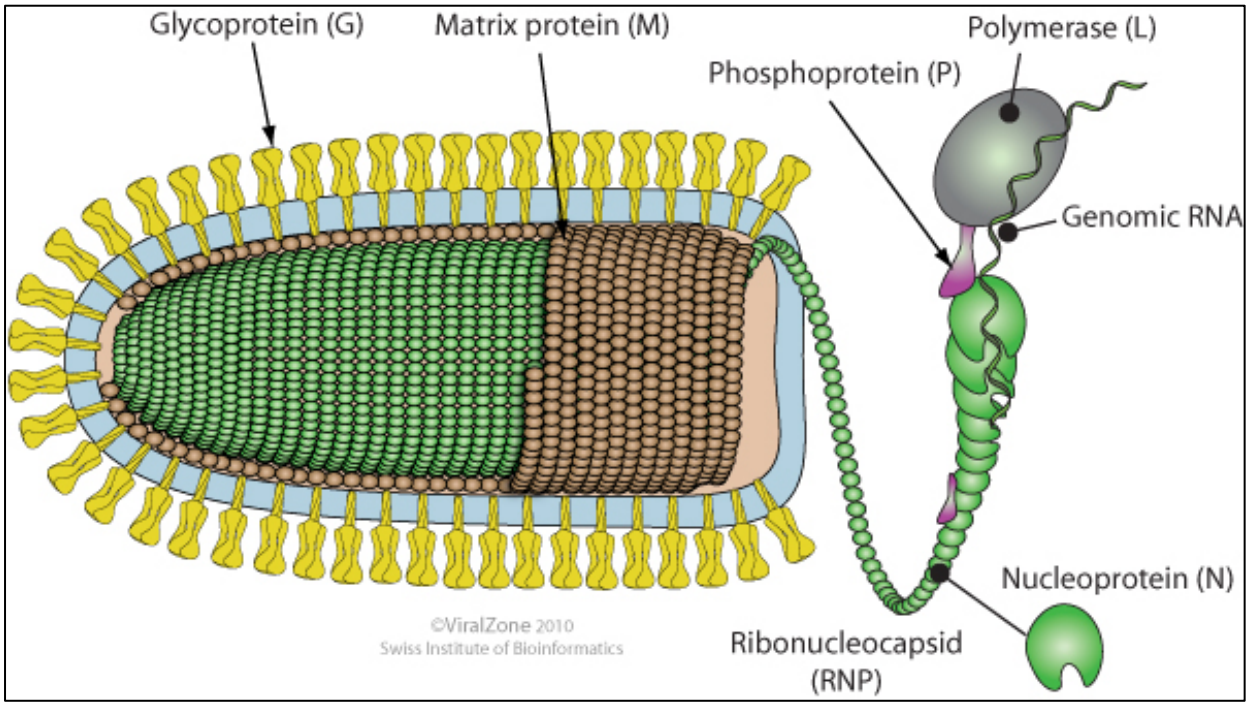

Figure 1. Diagram of VSV (ViralZone, SIB Swiss Institute of Bioinformatics)

The RNA genome is approximately 11 kb long and encodes 5 major genes in the following order: 3'- N – P- M – G – L – 5' (Figure 2). Transcription of the viral genome is polar and sequential, meaning there is a single transcription initiation site at the 3' end of the genome and transcription of each gene depends on transcription and termination of the gene immediately upstream. For example, transcription of the P gene is dependent on the proper transcription and termination of the N gene. This polar and sequential mode of transcription results in attenuation of viral transcription because the viral polymerase is more likely to fall off the genome as it travels farther from the 3'end. In other words, efficiency of transcription decreases with increasing distance from the 3'end of the genome. As a result, the N

monocistronic mRNA is the most abundant while much less L mRNA is transcribed. This transcriptional attenuation results in production of a gradient of viral proteins (4). On average, there is 20%-30% more of the previous protein than the one following it (3). The proportional generation of these proteins is extremely important, since changing the order, decreases viral fitness.

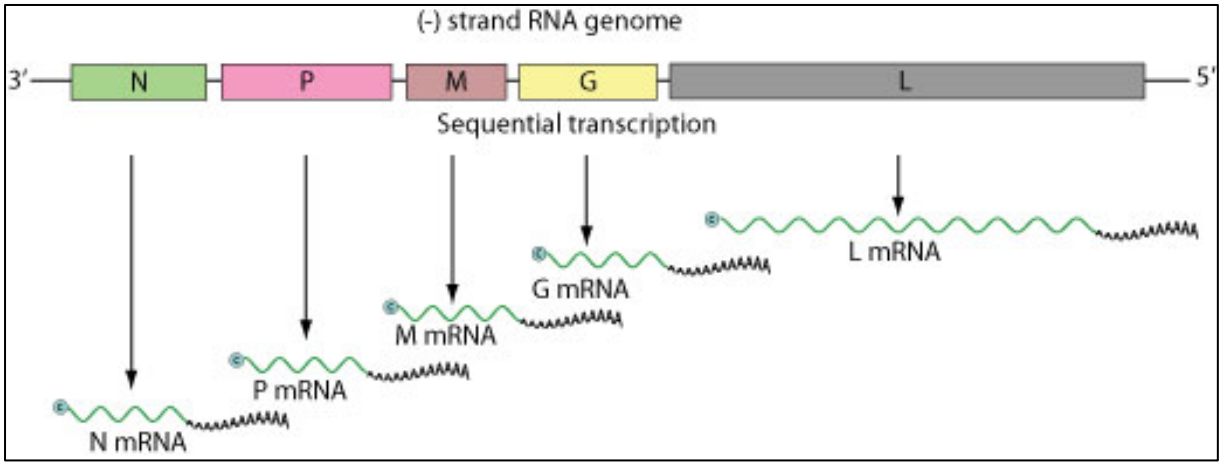

Figure 2. Vesicular stomatitis virus genome (ViralZone, SIB Swiss Institute of Bioinformatics)

The infectious cycle of VSV

Adsorption:

The infectious cycle begins with the pH dependent, adsorption of the virion via the G protein to the cell surface receptor (3). This receptor is thought to be the LDL receptor (LDLR) along with other members of the LDL family (5) This family of receptors is found on many cell types and explains why VSV has such a broad host range (5).

Penetration and uncoating:

The pH and temperature dependent process of virus penetration, proceeds through the cell membrane quickly via receptor mediated endocytosis (3). Next the virus is uncoated (also a pH dependent process), during which the input viral proteins are released into the cytoplasm (3).

Transcription:

VSV is a negative sense, single stranded RNA (ssRNA) virus, which means the genome is anti-sense to mRNA therefore the host ribosomes are unable to recognize the 5' end of the genome and initiate translation. First the viral polymerase must produce 5 monocistronic mRNAs from the input genome using a start and stop mechanism (Figure 3A). For example, the polymerase initiates transcription at the beginning of the N gene, generates a positive sense copy of the coding region, and then stops transcription at the end of the N gene and adds a modified cap and a polyA tail. The polymerase then reinitiates (starts) and the P gene and generates an mRNA encoding the P gene, which is capped and polyadenylated. As mentioned previously, transcription is polar and sequential, therefore once this process is complete, the polymerase

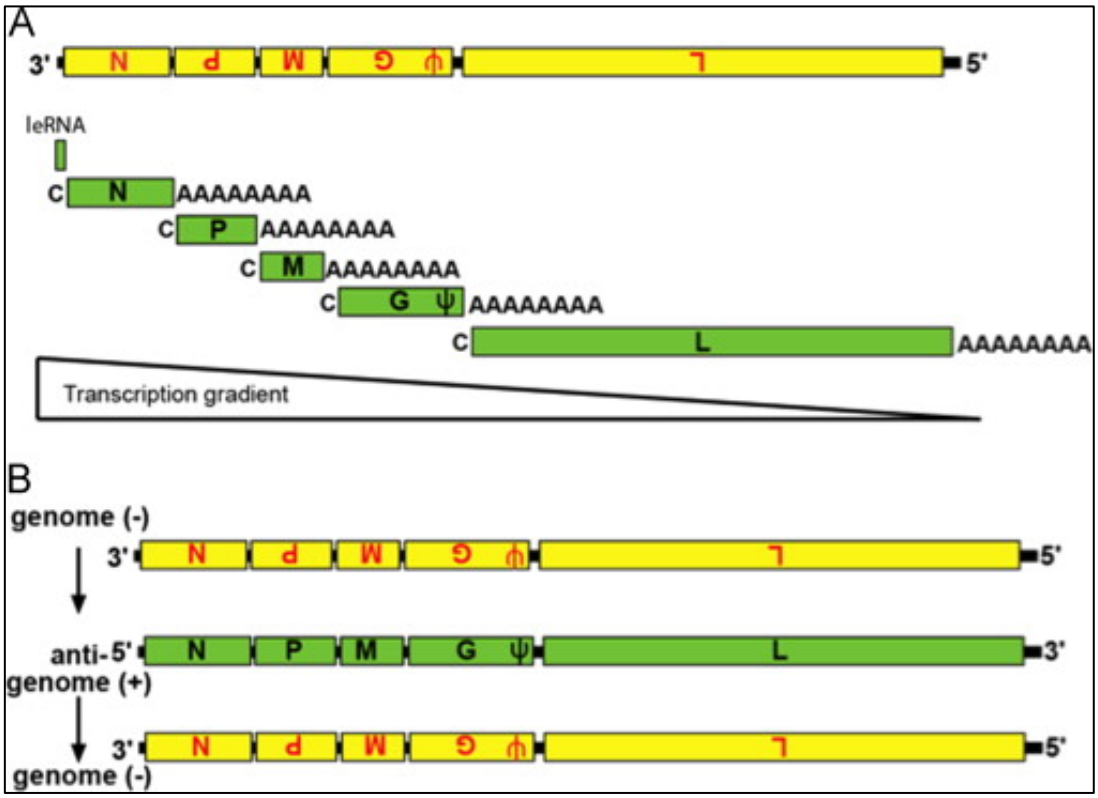

Figure 3. Transcription and Replication of VSV Genome (Adapted from reference (6) with permission)

has produced a gradient of capped, monocistronic, polyadenylated viral mRNAs that can be recognized by the host ribosomes and translated into viral proteins (3).

Replication:

Once enough viral proteins have been produced, the RNA polymerase switches gears and uses the input negative sense genomes as a template to generate full-length positive sense RNA anti-genomes. These positive genomes are then replicated by the polymerase into full length, negative sense molecules that will be packaged into virions as genomes during assembly (Figure 3B). An interesting question about the infectious cycle of negative sense RNA viruses is how the viral polymerase knows when to switch from transcription to replication. Evidence suggests that when the intracellular concentration of the N protein reaches a certain threshold, it will initiate the polymerase to create a template for the genomic RNA, thus beginning replication. This is logical as the amount of N is crucial since un-encapsidated RNA is rapidly degraded. This entire process of replication occurs within the cytoplasm of the host cell (3).

Assembly and Budding:

Post-translational glycosylation of G targets it for insertion into the cellular plasma membrane, where it functions as an “anchor” for the process of assembly. The M Protein binds with high affinity to membrane-bound G and then recruits the ribonucleoprotein cores (viral RNA plus N and lesser amounts of L and P) to join the complex, which are then released from the cell during a process called budding (3). This implies that the M protein is important for both assembly of the virion and eventual release of virions. The result of assembly and budding is the creation of a new bullet-shaped virion.

Type I Interferon Response

Type I interferons (IFN-α and IFN-β) are a crucial component of the innate immune system. These cytokines are considered the first line of defense against viral infection. In fact, IFNs are not active against other foreign bodies aside from viruses. For the purposes of this research, we will focus on IFN-β (IFN) which are known to induce an antiviral state in cells making them resistant to subsequent viral attack. Once the IFN response is activated, the IFN protein is produced and secreted outside the cell. It can then bind to IFN receptors on the cell surface of both the infected cell and uninfected, neighboring cells (Figure 4). This binding then activates a complex signal transduction cascade that results in the activation of over 300 genes that function to block overall protein production inside the cell and therefore limit production of viral proteins (7). In addition to creating an antiviral state in the cell, IFN induction also helps the host mount an adaptive immune response by activating lymphocytes (i.e. macrophages, T and B-Cells and natural killer cells) and antigen presentation cells (APCs) (8).

Induction of an IFN response

Inducers of the Type I IFN response are "pathogen-associated molecular patterns" (PAMPS). As illustrated in Figure 5, these inducers include double stranded RNA (dsRNA) which (7) can be produced by viruses as a replicative intermediate, and are recognized by "pattern recognition receptors" (PRRs) (8). There are several families of PRRs that induce IFN, which have been broken down into two main groups; toll-like receptors (TLR) and RIG-I like receptors (RLR). TLRs come in different forms to detect viral infection of the cell. TLRs are transmembrane proteins located on the intracellular endosomes membranes of many cells including leucocytes, macrophages, dendritic cells, cells of adaptive immunity, and some non-immune cells (9). TLR-3

binds to dsRNA, which is not commonly produced by mammalian cells and thus is an indicator of viral infection. TLR-7 binds to viral ssRNA found in the cytoplasm (7). Finally, TLR-4 has been known to bind to the G protein of VSV (7). The TLR-4 pathway eventually initiates responses by Interferon Regulating Factor 3 (IRF-3) and NF-κB, both of which are important transcription factors that must be activated before IFN can be produced (7).

RLRs are expressed in some immune cells and most non-immune cells (fibroblasts, myeloid and epithelial cells), and these receptors contain an RNA binding domain that recognizes virus-specific RNA within the cytoplasm. RIG-I, the prototypical molecule for this group, has been shown to detect in vitro transcribed dsRNAs. Another member, MDA5, which has a very similar composition to RIG-I, recognizes poly(I:C) which is a simulated dsRNA, but not the in vitro transcribed dsRNA. RNA viruses are also differentially recognized by RIG-I and MDA5 (10). Evidence suggests that RIG-I is the RLR that recognizes VSV RNA in infected cells (11), therefore the RIG-I dependent pathway is the focus of the work proposed here. As shown in Figure 5, once a RLR binds to viral RNA it triggers a signal transduction cascade that activates transcription factors (NF-κB, c-Jun, and IRF-3) that are essential for induction of early IFN-α gene expression (Figure 4) (2). Normally NF-κB family members are sequestered in the cytoplasm and tightly bound to Inhibitors of κB (IκBs), which keeps the molecule inactive by masking the nuclear localization signal (NLS). After RLR-dependent activation, the IκBs are degraded and the NLS on NF-κB is revealed, allowing it to be translocated to the nucleus where it can induce IFN mRNA production (12). The IFN mRNA is then translated into IFN protein, which as previously mentioned, is secreted outside the cell where it binds to its receptors on the surface of the infected and uninfected neighboring cells. This binding activates another

cascading pathway that induces the production of Interferon-stimulated genes (ISG), the formulation of which creates many hundred more products, including RIG-I, which in turn replicates the process in a positive feedback loop (7). RIG-I knockout mouse fibroblast cells show that IFN production was diminished following VSV infection, which led to a 1.5 log increase in viral titers observed in these test mice (7).

Viral Evasion of the IFN Response

To combat this extremely effective form of defense, viruses have developed ways to circumvent the host's IFN response. For example, some viruses have evolved mechanisms to hide their RNA from RIG-I such as post-translational modification (PTM) of the RNA, competitive viral protein binding, and sequestering RNA into organelles other than the cytoplasm (11). Influenza A and Ebola virus (EBOV) use a sequestering method to hide its RNA from PRRs, though the mechanism varies (13).

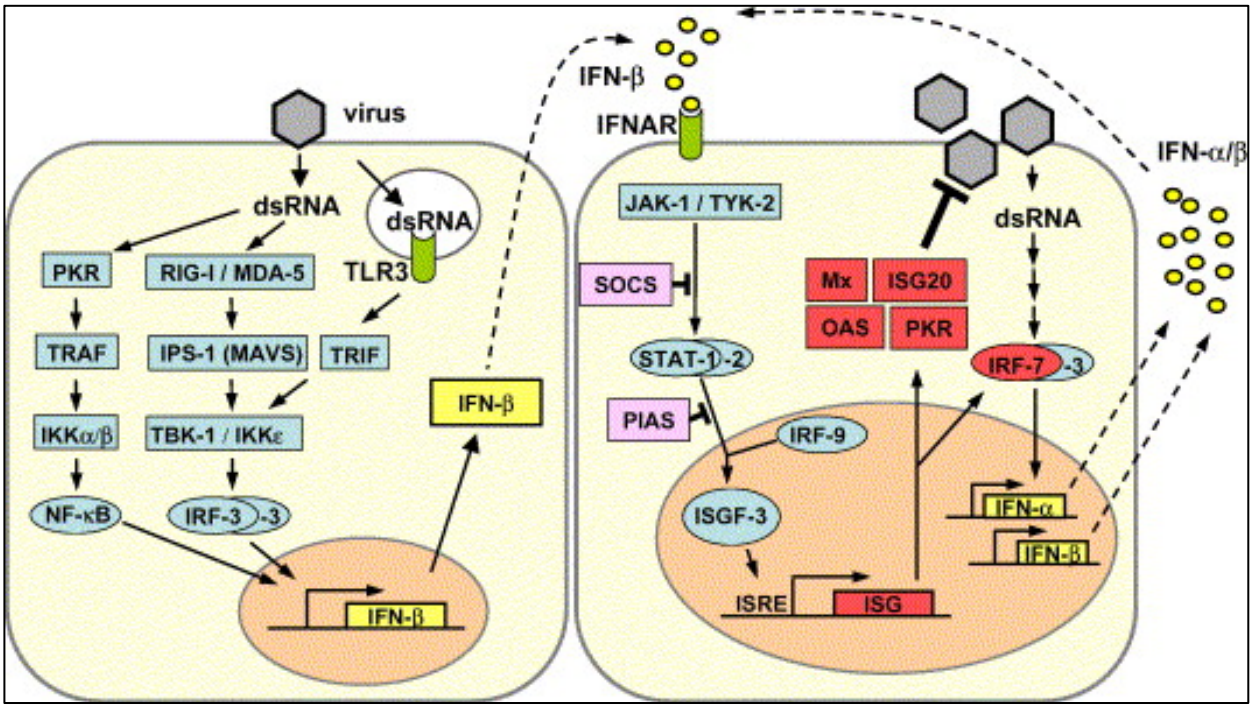

Figure 4. Interferon pathway (Adapted from reference (2) with permission)

VSV and the IFN Response

VSV is exquisitely sensitive to the effects of IFN-β. In fact, one molecule of IFN is sufficient to block successful VSV infection (14). In response, VSV also has its own methods of evading the IFN response. It is believed that the M protein is the most active participant in evasion of the IFN response within VSV-infected cells. VSV strains that encode an N-terminus mutation in M protein that changes a methionine to an arginine at position 51 [M(M51R)] are not able to inhibit host gene expression or suppress the IFN response, however viruses encoding this mutation are still able to effectively replicate and assemble virions (7, 15). Research indicates that the M protein alone can down-regulate host mRNA production, since it is sufficient to inhibit nuclear export of mRNA even in the absence of other VSV proteins (7). The M protein is

also able to inhibit the host RNA-dependent polymerase II (16). It has been postulated that VSV inhibits host gene expression by binding to and interfering with the function of Rae1 and nucleoprotein Nup98, cellular components of the nuclear pore that are required for mRNA transport to the cytoplasm (7). These two nuclear pore proteins are complexed in the cell, and M binding to Nup98 is indirectly mediated by Rae1. Further study is necessary to determine the whether this binding has a direct impact on gene expression (7). An important mutant strain for this research has been T1026R1 (R1), which encodes the M(M51R) mutation. Infection with R1, as well as other strains encoding this mutation in M, results in induction of a robust IFN response, however these viruses are delayed in their ability to inhibit host gene expression. Due to these correlated activities, it has been hypothesized that the IFN response is suppressed because M limits global host gene expression (17).

Project Foundation

It is believed that M limits the IFN response through its ability to inhibit global host transcription (18), while others propose that the M protein also inhibits NF-κB, which in turn abrogates IFN expression through downstream suppression (12). This belief is based on the following: (1) M inhibits virus-mediated NF-κB activation when expressed during infection or independently, (2) the M(M51R) mutation found in R1 abrogates this function, and (3) M targets a step upstream of the IκB kinase (IKK) in the canonical NF-κB activation pathway. These findings indicate that there may be two independent abilities of M involved in the abrogation of IFN response. One is the ability of the M protein to inhibit global host transcription and the second is the blocking of NF-κB activation, through which, the VSV M protein evades the RIG-I dependent pathway that leads to IFN gene expression (Figure 5).

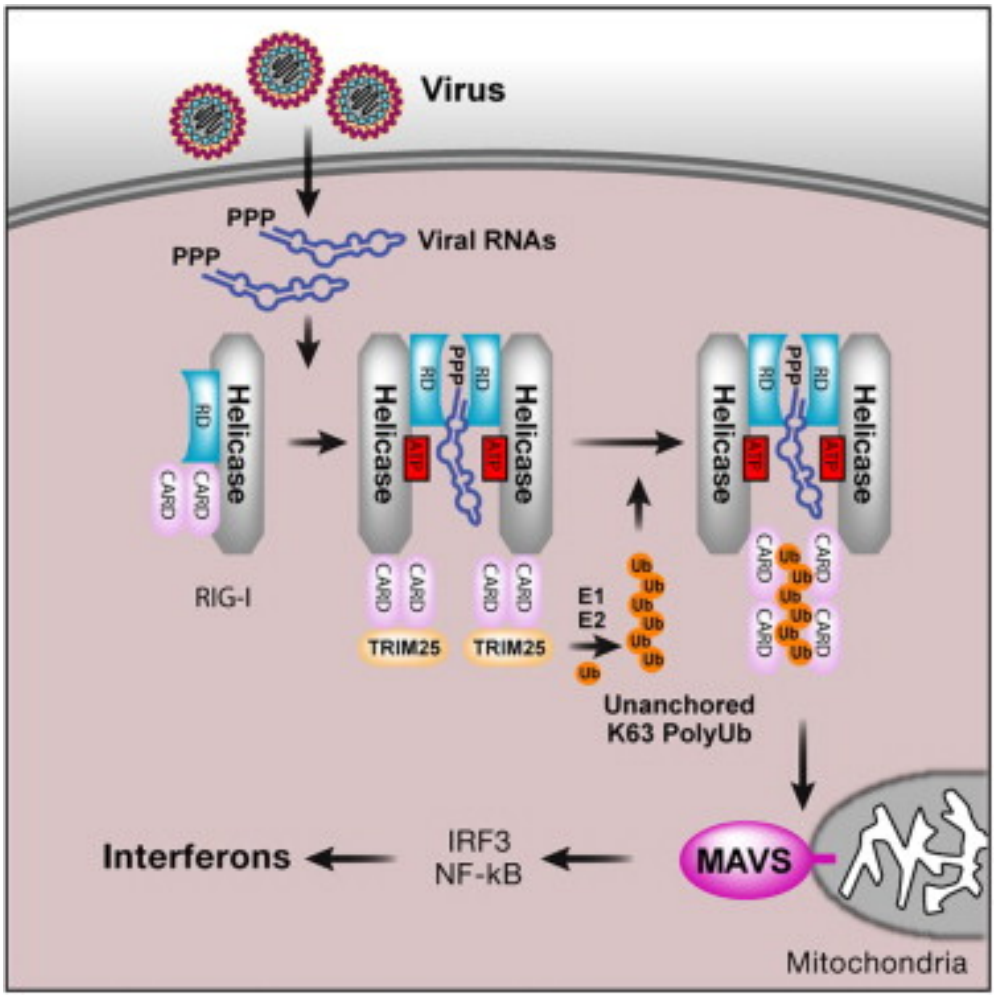

Figure 5. RIG-I pathway during infection. (Adapted from reference (1) with permission)

However, another study shows that the M protein is not involved in suppression of the IFN response in chicken-embryo cells (CEC) (14). Researchers compared the IFN-inducing capacity of 36 plaque-derived subpopulations of field isolate VSV-IN no. 22 and found that only isolate 22-20 was an excellent inducer of IFN, while its sister plaques induced little to no IFN in these cells. Interestingly, genome sequencing determined that the M gene of 22-20 was identical to another sister isolate, 22-25 (14). Since CEC are sensitive to the effects of the M protein on host transcription (19), it was concluded that the M protein does not play a role in suppression of

the IFN response by VSV. These results could be explained if two viral functions, M-mediated inhibition of host transcription and regulation of an early step in IFN gene induction, are involved in regulation of IFN gene expression. While VSV mutant R1 may be defective in both functions, isolate 22-20 may be defective in only one - the one responsible for limiting IFN induction at an early step of transcription. As described above, it has been reported that in addition to inhibiting host gene expression, the M protein prevents activation of NF-κB (12). To determine if 22-20 is indeed defective in an early step of IFN gene induction, 22-20 and 22-25 have been further characterized. To begin, the genomes of both viruses were sequenced.

A single coding mutation was identified in the M gene of 22-20, which changed the highly conserved aspartic acid residue at position 52 of the M protein to a glycine [M(D52G)]. Interestingly, this mutation is located one amino acid away from the M(M51R) mutation found in R1. It was also determined that both 22-20 and 22-25 inhibited host gene expression, indicating that the M(D52G) mutation did not perturb this function of M. Immunofluorescences studies show that 22-25 prevents activation of NF-κB, while 22-20 activates this transcription factor. Finally, little to no IFN mRNA or IFN protein was detected in 22-20 or 22-25–infected cells; likely due to M-mediated inhibition of host gene expression. The researchers posit that the M51R mutation in R1 M results in a virus that is defective in two functions, inhibition of NF-κB activation and host gene expression, while the M(D52G) mutation in 22-20 results in a virus that is only defective in an early step of IFN gene induction, preventing NF-κB activation (Table 1).

Table 1. VSV Functional Differences.

Virus	M Protein Mutation	Transcription Inhibition (M protein)	NF-κB activation suppressor	Host Transcription Inhibited	NF-κB Activated	IFN gene expressed
wt	None	Functional	Functional	Yes	No	No
R1	M51R	Defective	Defective	No	Yes	Yes
22-25	None	Functional	Functional	Yes	No	No
22-20	D52G	Functional	Defective	Yes	Yes	No

The overall goal of this work is to use RNA-Seq to investigate host genome expression in mouse L929 cells infected with 22-20 or 22-25. As both viruses inhibit global host gene expression, this comparative transcriptome analysis will identify differentially expressed genes (DEG) that are involved in NF-κB activation and identify this and other host pathways that are perturbed during early VSV infection. There seem to be few M protein mutations that abrogate one cytopathic effect of the VSV M protein, while maintaining the ability to inhibit host gene expression. Therefore, comparing this set of viruses offers a unique opportunity to understand the actions of M protein during initial infection. This includes identifying which genes involved with the NF-κB response are differentially expressed and ascertain the effect that the M protein may have on host pathways during infection. RNA-Seq will allow us to determine the effect of the [M(D52G)] mutation on the ability of M protein to abrogate the IFN response while still inhibiting host transcription.

Broader Impacts

VSV has become increasingly attractive as a platform for the generation of recombinant viral vaccines for several reasons: (1) the general human population lacks antibodies to the virus; (2) human infections are rare and when they do occur the symptoms are mild; (3) the virus is not genotoxic; (4) replication occurs in the cytoplasm therefore insertion into the host genome is not a concern; (5) the virus is amenable to editing thanks to the development of a reverse genetics system to create recombinant viruses (20). Recombinant VSV has already been used as a vaccine vector for deadly viruses such as Marburg and Ebola virus (21). The Ebola virus vaccine made with recombinant VSV (rVSV-ZEBOV) has gone through phase 1 and 2 trials, with minimal side effects (22). A more recent test in Guinea, Africa showed that, after thousands of tests with the pseudotyped VSV, not one patient became infected with the Ebola virus (23). It has also been shown that, using a booster type immunization, pseudotyping VSV with the glycoprotein of lymphocytic choriomeningitis virus (VSV-GP), has circumvented the rapid creation of antibodies against the wt VSV, making it an even better viral vector (20).

For many of these same reasons, researchers are trying to use VSV as an anticancer agent. VSV, and several other viruses are being considered for this type of therapy, creating the burgeoning field of oncolytics; the use of certain viruses to selectively destroy cancer cells. The majority of human cancer cells lack an IFN response, making infection by mutant M51R VSV more likely (24). This, in turn, will produce cell death by apoptosis, leading to tumor reduction. Healthy cells can mount a much more robust immune response, keeping them safe from harm.

Materials and Methods

Cells, viruses, and infections

Monolayer of mouse fibroblast L929 (ATCC CCL-1) were grown in complete media containing Eagle's Minimum Essential Medium (EMEM) supplemented with 10% Horse Serum (HS). VSV field isolates 22-20 and 22-25 were generous gifts from Philip Marcus (University of Connecticut) and have been previously described. The heat resistant strain of the Indiana serotype of VSV was used as the wild type (wt) virus (31, 32). All viruses were grown on either baby hamster kidney cells or Vero cells as previously described (33). Cells were infected with each virus at a multiplicity of infection (MOI) of 5 PFU/cell unless otherwise stated. Virus was adsorbed in MEM for 3 h at 37 °C in the absence of serum.

RNA Isolation

Total RNA was isolated from infected L929 cells at 1 hour and 3 hours post infection (hpi) using the TRIZol Plus RNA Isolation Kit (Life Technologies) according to the manufacturer's directions. To ensure that the highest quality RNA is used in this analysis, 4 biological replicates of each condition were isolated. RNA was quantitated via nanodrop and bioanalyzer. For each condition, the 2 highest quality samples were used for RNA-Seq.

RNA-Seq

Full workflow integrated service (RNA-Seq through Data QC and Analysis) was provided by ProteinCT Biotechnologies (Madison, WI). Complementary DNA (cDNA) libraries were prepared using the Illumina TruSeq strand specific mRNA sample preparation system (Illumina). Briefly, mRNA was extracted from total RNA using polyA selection, followed by RNA fragmentation.

Strand specific libraries were constructed by first-strand cDNA synthesis using random primers, sample cleanup and second-strand synthesis using DNA Polymerase I and RNase H. A single 'A' base was added to the cDNA fragments followed by ligation of the adapters. Final cDNA library was achieved by further purification and enrichment with PC. The quality of the cDNA library was checked using the Agilent 4200 TapeStation. The libraries were sequenced (Single end 100bp reads) using the Illumina HiSeq4000. Ten samples per lane were run, with final counts reaching over 20 million reads per sample.

Data QC and Analysis

The fastQC program was used to verify the quality of the raw Illumina reads. The GRCm38 (mm10) mouse reference genome and Ensembl gene annotations (v82) were used for read mapping. The raw sequence reads were mapped to the reference genome using Subjunc aligner from Subread (25), with majority of the reads (over 90% for all samples) aligned to the genome. The output from Subread is a BAM file (.bam). This is the binary version of a SAM file (.sam), which, in turn, is a tab-delimited text file that contains sequence alignment data. The alignment BAM files were compared against the gene annotation general feature format (GFF) files. GFF files (.gff) are formatted to describe multiple features of DNA, RNA and protein sequences. Following comparison, the raw counts for each gene were generated using the featureCounts tool from Subread, with over 90% of reads overall assigned to genes. The raw counts data were normalized using the voom method from the R Limma package (26). Based on the differential expression of genes, further analyses were carried out to detect enriched biological functions.

Internal RNA-Seq Workflow

This workflow closely follows the pipeline outlined in Pertea et. al. (27) with modifications. The HISAT2 aligner software was used to map the raw data from the Illumina reads that was provided by ProteinCT to the GRCm38 genome (with annotations for single-nucleotide polymorphisms (snps) and transcripts) (28). This aligner also provided a high rate of alignment, ranging from 85.16% - 95.16%. SAMtools (29, 30) was then used to convert the SAM output files from HISAT2 into BAM files. These converted files were subsequently compared to the Ensembl gene annotations (v90) GTF file using Stringtie (31). These gene assignments were also well above 90%. The Stringtie output (estimated counts) were then converted to raw counts to use as input for differential expression analysis using R Bioconductor packages.

Differential Expression and Biological Pathway Analysis

This section of the workflow closely follows that described in Law et. al. (32) with modifications. The raw read counts were normalized using the edgeR package and the voom method in R Limma package (26, 33, 34). Subsequently, the differential expression of genes was analyzed. Enrichment analysis, including gene set testing and specific pathway enrichment, was completed using the camera and kegga methods respectively from the R Limma package. Visuals for pathway enrichment and gene expression were created using the R Pathview package (35).

Results

Multidimensional Scaling

Multidimensional scaling (MDS) of the transcriptome data was performed to determine sample relationship similarity (Figure 6). The MDS plot suggests that the technical replicates cluster closely together, indicating that this experiment should yield reliable results. This plot further indicates that gene expression in mock (1 hpi) and 22-20 (1 hpi) are similar, indicating that

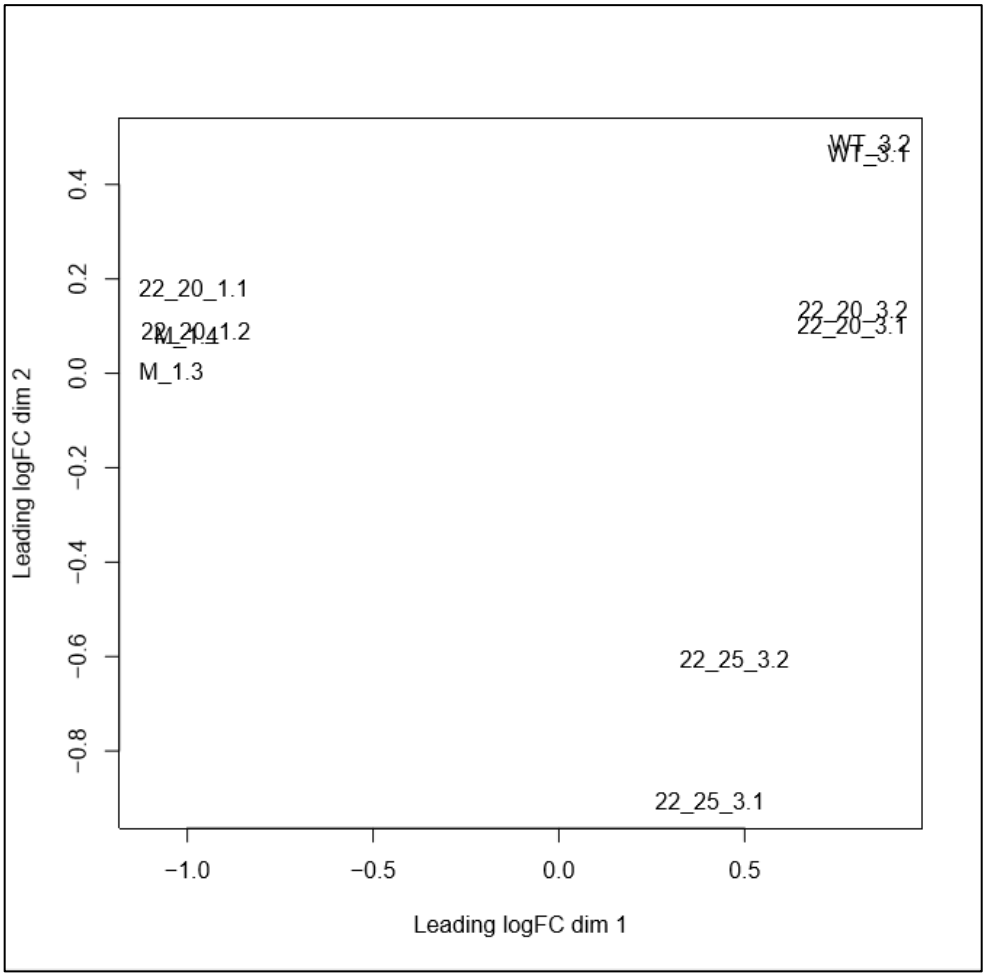

Figure 6. Multidimensional scaling (MDS) plot of the transcriptome data to identify sample clustering patterns. Number after the underscore represents the hours after infection (1 or 3 hr.) followed by the replicate number. Leading logFC dim 1: First MDS component (X-Axis); Leading logFC dim 2: Second MDS component (Y-Axis). Plot was generated via the edgeR package

there is not much change in host cell gene expression within the first hour of infection. Likewise, of the 3 hpi samples, wt and 22-20 are more “related” to each other and 22-25 is the most different. Overall, samples from different groups are well separated. Consequently, each biological group (virus strain) clustered closely together and each condition (time), separate from each other (Figure 6).

Heatmap Analysis

Variable analysis of the top 100 DEGs confirmed the trends in clustering of samples observed in the multidimensional scaling (Figure 6). The analysis of the “top 100 DEG” illustrates the differences in host gene expression between the infections at 3 hpi versus the mock infected cells and even the infections at 1 hpi (Figure 7). Furthermore, a large number of genes in this subset are down regulated in response to viral infection by the group at 3 hpi than those at 1 hpi.

This clustering of 1hpi and 3hpi genes, can also be seen with 1093 DEGs (Figure 8). Furthermore, although our analysis and that of Protein CT used different parameters were used by internal analytics to obtain gene subsets, this study confirms the groupings and patterns of ProteinCT, even when considering clustering remains similar between a small subset (Figure 7) and a large one (Figure 8). Biological groups clustered together, with 22-20 (1 hpi) associating with Mock (1 hpi) and 22-20 (3 hpi) with wt (3 hpi). We also notice that the three infections at 3 hpi are more similar than the earlier infections, as is expected based on the previous results (Figure 8). When considering the number of genes used in the ProteinCT overall heatmap, we increased the number of genes in our analysis to 1500. The intention here was verify whether

our analytical pipeline would provide similar results. We summarily found that our internal analysis confirms this clustering of genes through variable analysis of the "top 1500 DEG" (Figure 9) which were obtained using parameters similar to the "top 100 DEG" (Figure 7).

Venn Diagram Comparison

Further analysis finds that 12.99 %, of the overall number of genes (15,556), are similar between the following three comparisons: 22-20 (3hpi) versus Mock; 22-25 (3hpi) versus Mock, wt (3hpi) versus Mock (Figure 10). There are, however, far more genes that are differentially expressed that are in common between the wt and 22-20 viruses than between wt and 22-25 viruses (869 versus 87, respectively). This demonstrates the association between 22-20 and wt and may explain their clustering in both MDS and heatmap analyses (Figures 6-9). 22-20 maintains 508 differentially expressed genes in common with 22-25, independent of those in common with wt. 19 genes were found to be differentially expressed between 22-20 and wt (7 up regulated, 12 down regulated, adjusted p- value < 0.05) (Figure 11). Of the 2528 genes in common between 22-25 and 22-20, 137 total genes were found differentially expressed (71 upregulated, 66 downregulated, adjusted p-value < 0.05) (Figure 12). Here, we notice that distinct groups of genes seem to be up or downregulated between 22-25 and 22-20 just as can be seen between 22-20 and wt. It was also discovered that within the 22-25 versus 22-20 comparison, both hallmark gene sets for interferon alpha and gamma response were down regulated (Table 2). This suggests that 22-25 downregulates both IFN Type I and IFN Type II pathways, when compared to the effects of 22-20. Furthermore, it is evident that far more genes in this gene set were downregulated by 22-25 than by 22-20 (Figure 13). Of the genes found in this gene set, 5 - Cxcl10, Irf9, Ifit3, Gbp2, Rsad2 - were found to be differentially

expressed (adjusted p-value < 0.05) (Table 3). All 5 of these genes had a negative log fold change (logFC) indicating downregulation.

KEGG and Gene Ontology Analysis

KEGG pathway analysis reveals that several important pathways, including NF-κB, RIG-I, Autophagy and Apoptosis, include differentially expressed genes (Figures 14 – 21). 21 genes in the NF-κB pathway were found to be differentially expressed (FDR < 0.05) by 22-20 (3hpi) versus Mock (1hpi) with 8 upregulated and 13 downregulated (Table 4). This follows a trend which indicates an overall down regulation of the pathway (Figure 14). The differences in the induced gene expression for this pathway between 22-25 and 22-20 appear to consist of further down regulation. Interestingly, there were no significant variations (adjusted p-value < 0.05) found between 22-25 (3hpi) and 22-20 (3hpi) for the NF-κB pathway.

In the RIG-I pathway, 10 genes were found to be differentially expressed (adjusted p-value < 0.05) in 22-20 (3hpi) versus Mock (1hpi) with 4 upregulated and 6 downregulated genes (Table 5). Again, there appears to be larger amount of down regulation of genes than up regulation regarding 22-25 versus 22-20 (Figure 17). In this instance, one gene, Cxcl10/IP10, was found to be significantly downregulated between 22-25 (3hpi) and 22-20 (3hpi).

We also found 36 DEG in the Apoptosis pathway (adjusted p-value < 0.05) in response to 22-20 (3hpi) versus Mock (1hpi) with 12 upregulated and 24 downregulated (Table 6). By comparison, 3 DEG were found in response to 22-25 (3hpi) versus 22-20 (3hpi), all of which exhibited upregulation. Two of these genes, Mcl1 and Atf4, were found to be significantly expressed by 22-25 and 22-20, an occurrence that was unique to the apoptosis pathway.

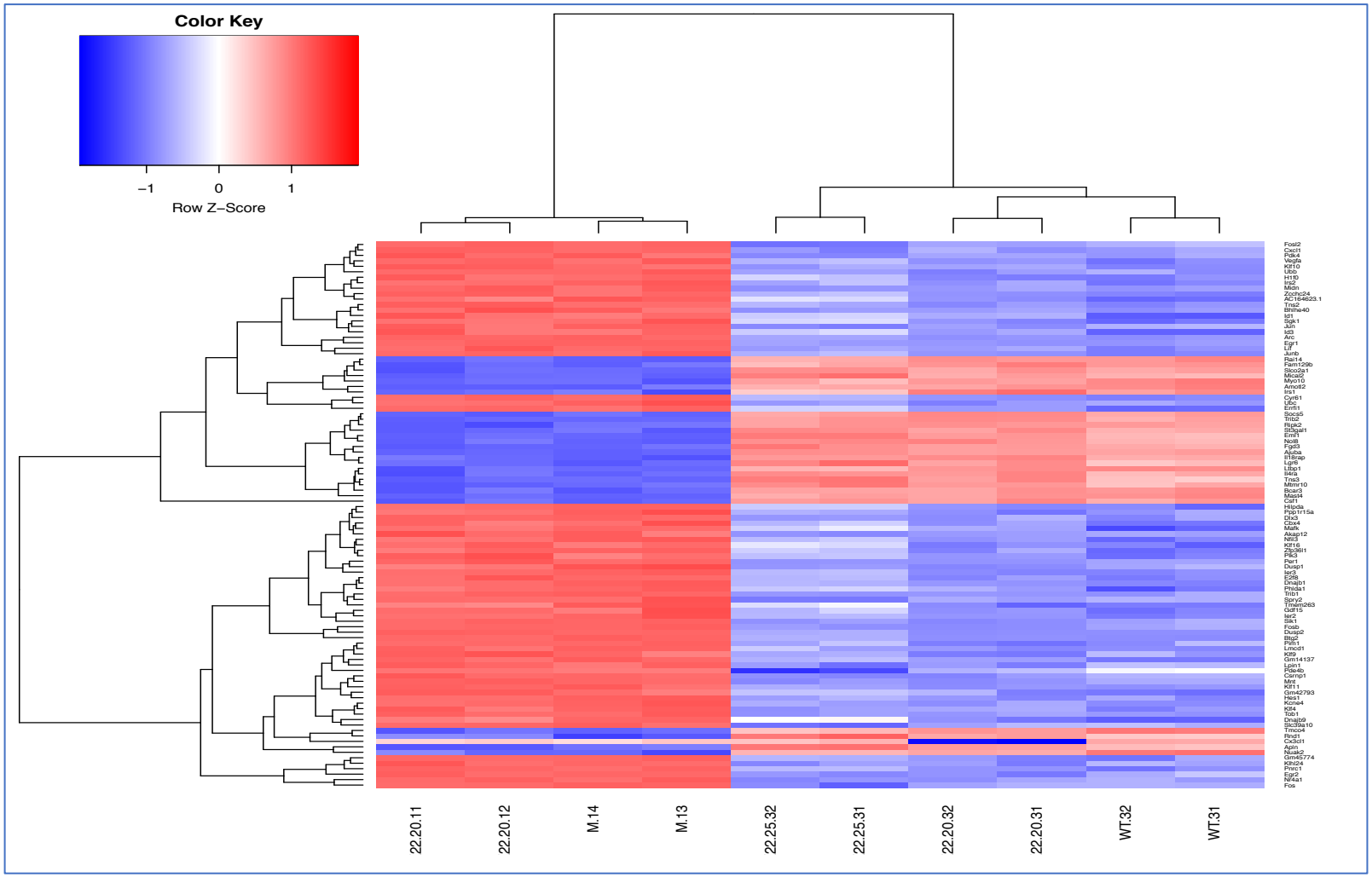

Figure 7. Variable comparison of the Top 100 genes that are differentially expressed in VSV-infected L929 cells (RIT Internal Analysis). A subset of the top 100 DEGs were selected (based on an adjusted p-value <0.05) from the comparison between 22-20 (3 hpi) and Mock. The genes were sorted based on adjusted p-value, smallest to largest. The expression values for these same genes were analyzed across all samples and normalized to standard deviation units (z-score) by row (genes). Red: increased expression, blue: decreased expression. The dendrogram at the top of the heatmap displays the hierarchical clustering of the virus sample replicates. The dendrogram to the left of the heatmap displays the hierarchical clustering of genes, with gene names shown along the right side of the heatmap.

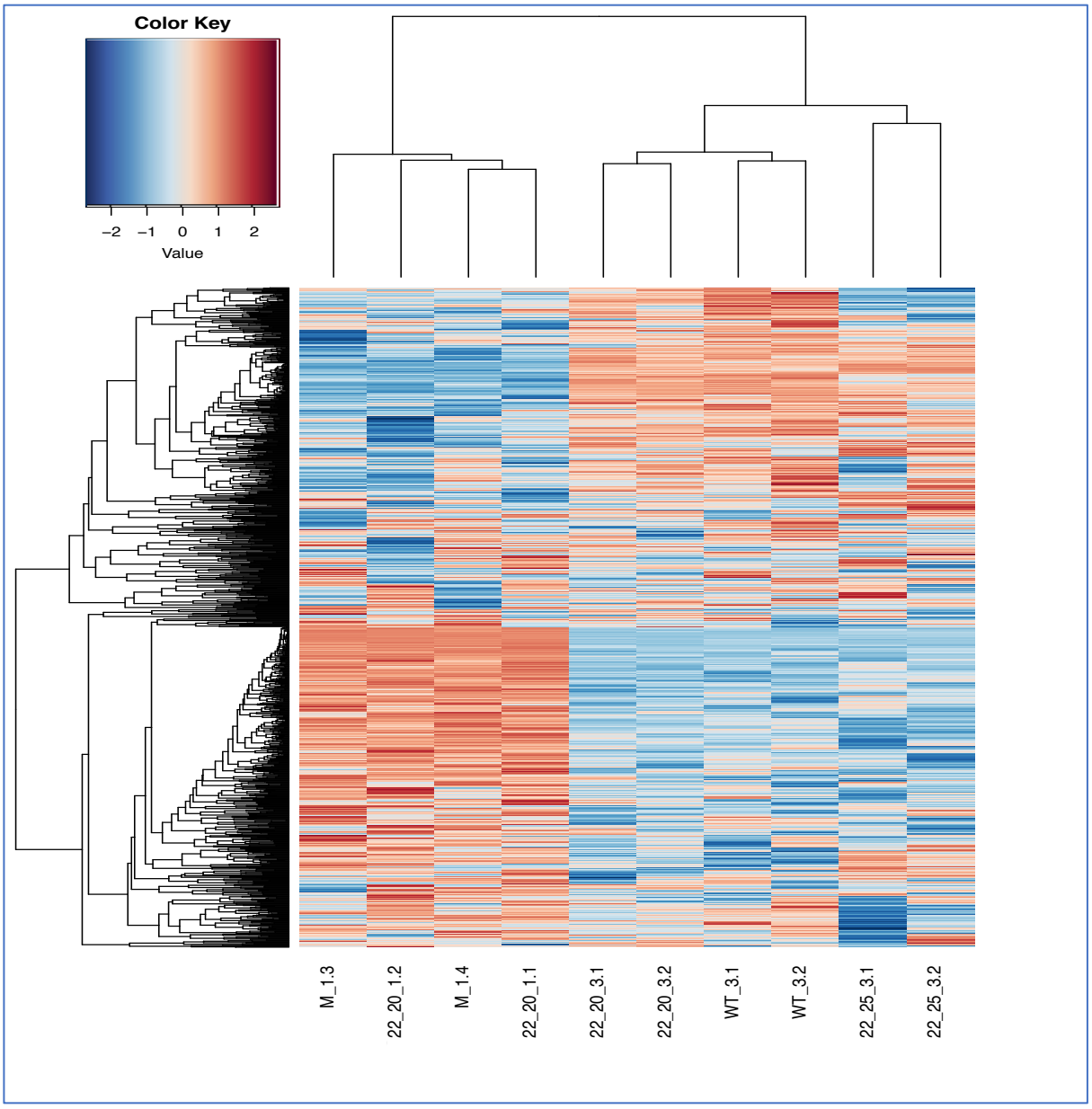

Figure 8. Variable comparison of the "overall top genes" that are differentially expressed in VSV-infected L929 cells (ProteinCT). The genes were selected based on the following parameters: a standard deviation (SD) of expression values larger than 30% of the mean expression values (Mean) and had a mean log counts-per-million (logCPM) > 1. These parameters were chosen to define the most significantly expressed genes within the experiment. 1093 genes met these criteria and were plotted against all samples. Red: increased expression, blue: decreased expression. The dendrogram at the top of the heatmap displays the hierarchical clustering of the virus sample replicates. The dendrogram to the left of the heatmap displays the hierarchical clustering of these genes.

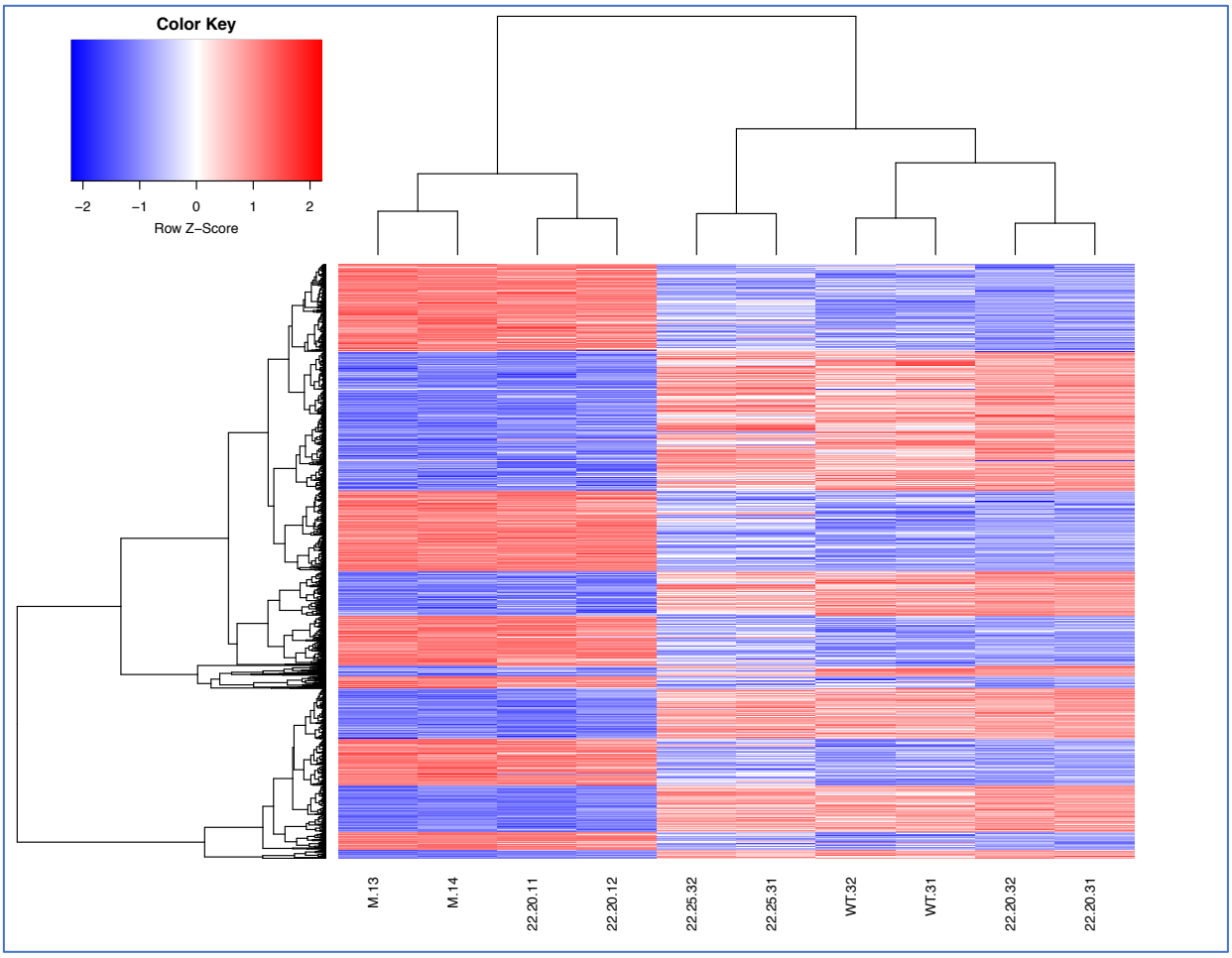

Figure 9. Variable comparison of the top 1500 genes that are differentially expressed in VSV-infected L929 cells (RIT Internal Analysis). DEGs were selected based on an adjusted p-value < 0.05. The genes were sorted based on adjusted p-value, smallest to largest. A subset of the top 1500 genes were selected from the comparison between 22-20 (3 hpi) and Mock. The expression values for these same genes were analyzed across all samples and normalized to standard deviation units (z-score) by row (genes). Red: increased expression, blue: decreased expression. The dendrogram at the top of the heatmap displays the hierarchical clustering of the virus sample replicates. The dendrogram to the left of the heatmap displays the hierarchical clustering of these genes.

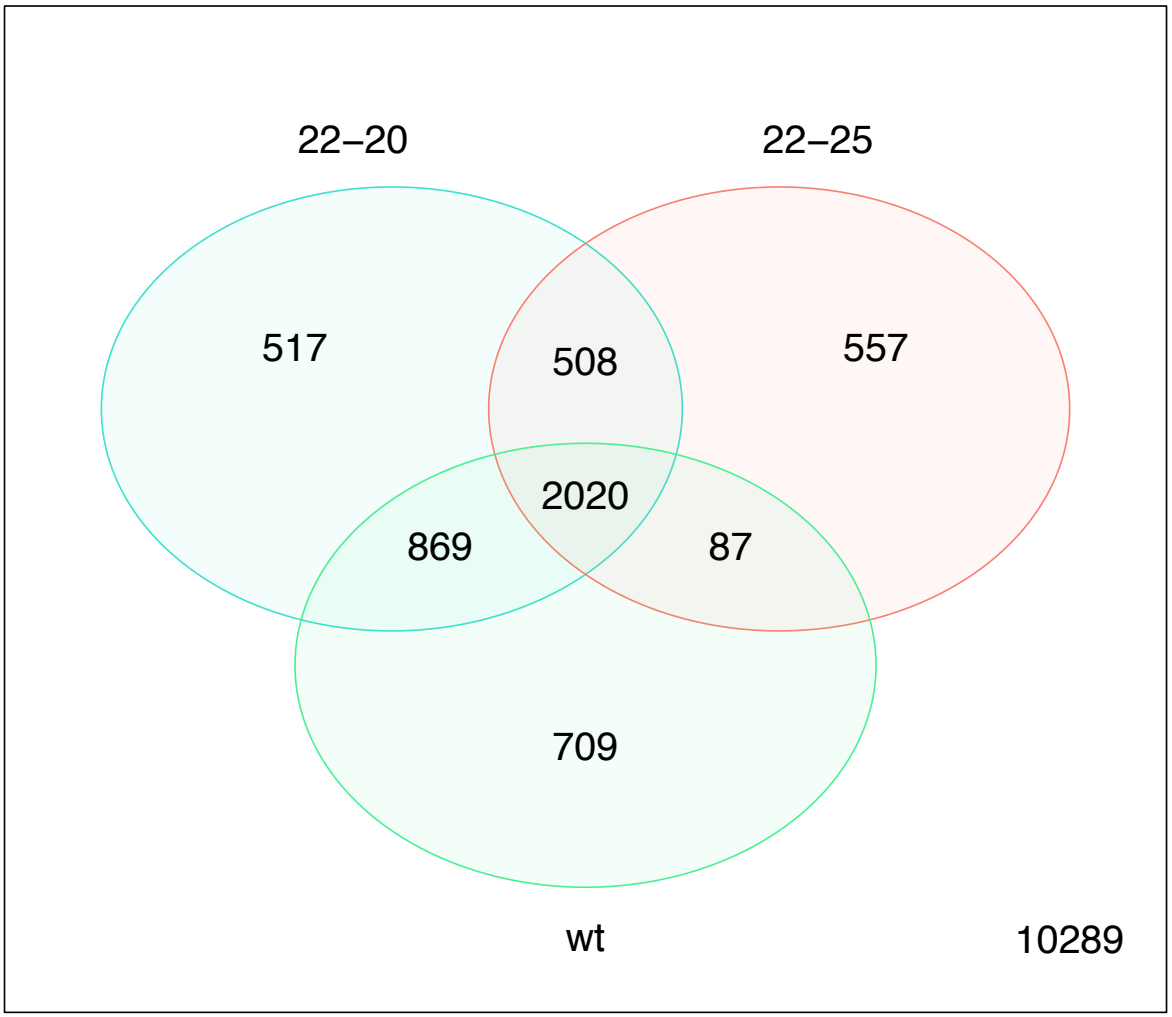

Figure 10. Venn Diagram of Viral-Modulated Gene Expression. The mRNA differential expressions of wt or mutant M viruses relative to mock-infected cells are depicted in three overlapping circles. DEGs were selected based on a cutoff adjusted p-value < 0.05 which includes both up and downregulated genes. The numbers indicate the mRNA counts in the indicated area. The number of genes not found significant is 10289 (lower right-hand corner).

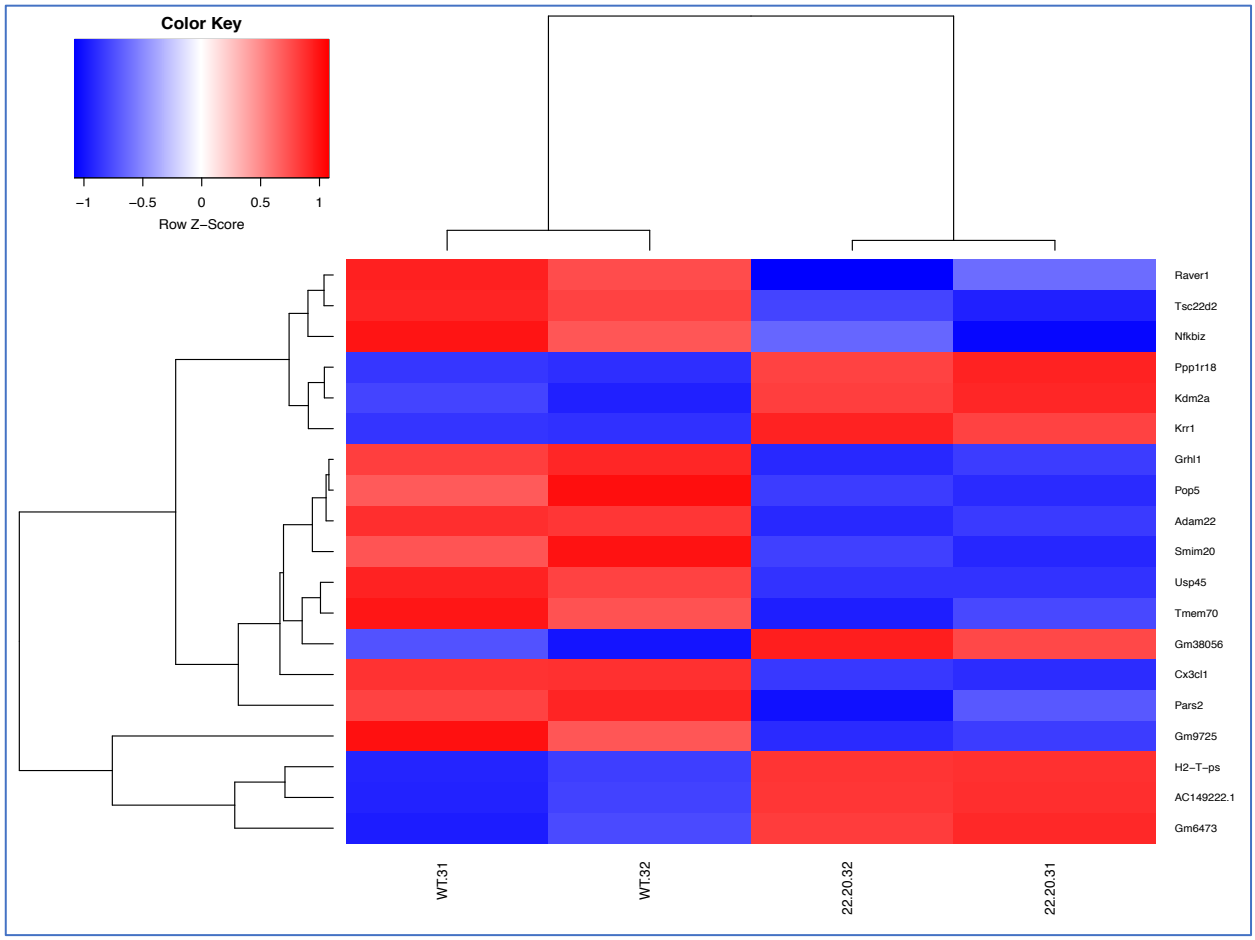

Figure 11: Variable comparison of DEGs between 22-20 (3 hpi) and wt (3 hpi) infected L929 cells. DEGs were selected based on an adjusted p-value < 0.05. Those genes that passed this cutoff, were selected from each sample within the group comparison of 22-20 (3 hpi) and wt (3 hpi). The expression values for these same genes were analyzed across all samples and normalized to standard deviation units (z-score) by row (genes). Red: increased expression, blue: decreased expression. The dendrogram at the top of the heatmap displays the hierarchical clustering of the virus sample replicates. The dendrogram to the left of the heatmap displays the hierarchical clustering of genes, with gene names shown along the right side of the heatmap.

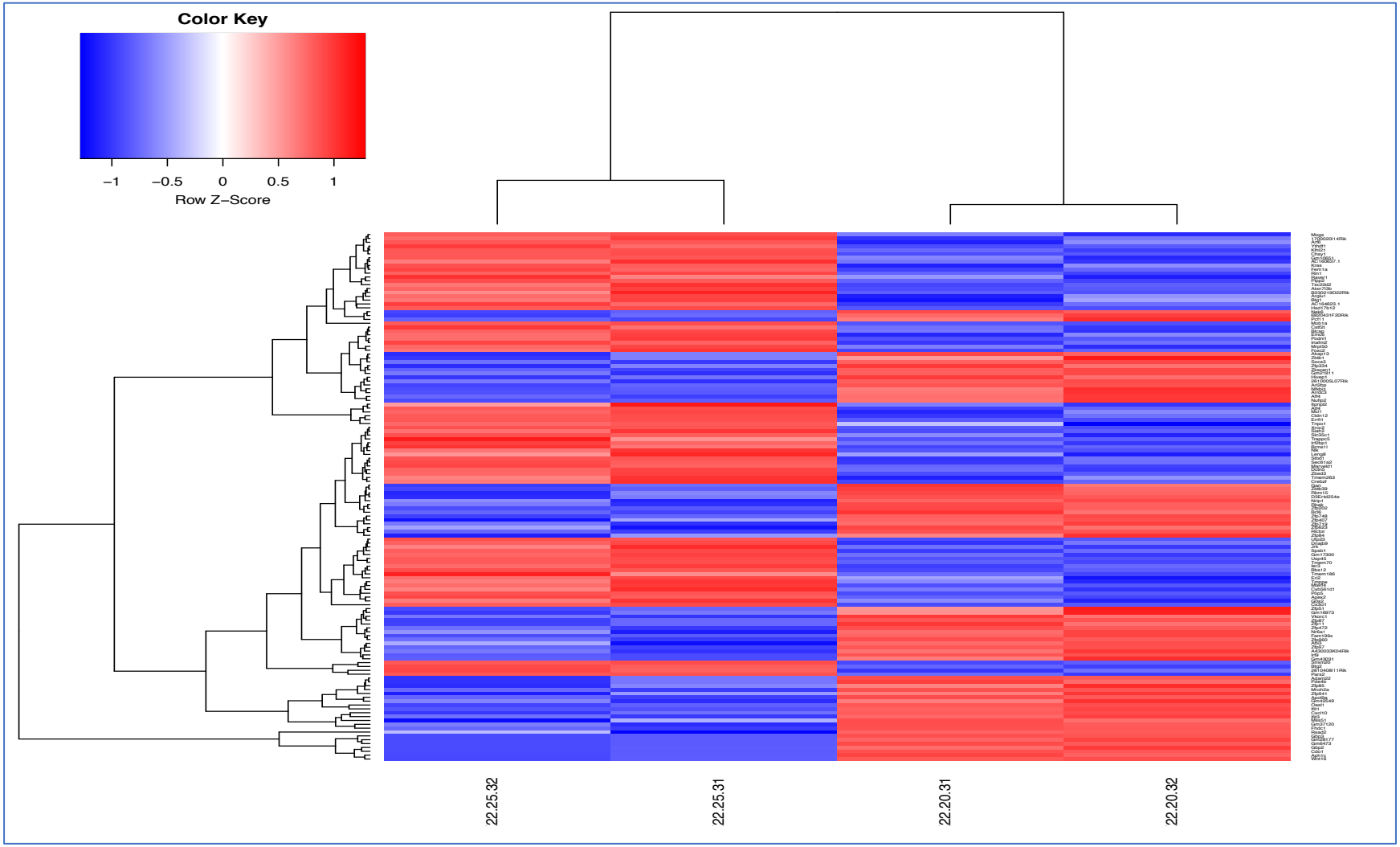

Figure 12. DEGs between 22-25 and 22-20. DEGs were selected based on an adjusted p-value < 0.05. Those genes that passed this cutoff, were selected from each sample within the group comparison of 22-25 (3 hpi) and 22-20 (3 hpi). The expression values for these same genes were analyzed across all samples and normalized to standard deviation units (z-score) by row (genes). Red: increased expression, blue: decreased expression. The dendrogram at the top of the heatmap displays the hierarchical clustering of the virus sample replicates. The dendrogram to the left of the heatmap displays the hierarchical clustering of genes, with gene names shown along the right side of the heatmap

.

Table 2: 22-25 (3 hpi) versus 22-20 (Gene Set Testing). DEGs within the comparison of 22-25 (3 hpi) and 22-20 (3 hpi) were matched to hallmark gene sets found in the Molecular Signatures Database (MSigDB). Hallmark gene sets with a false discovery rate (FDR) < 0.05 were selected via camera method in Limma. Gene Set: Name of gene set from MSigDB; NGenes: Number of genes in the set; Direction: Direction of differential expression (e.g. "Up" or "Down"); Pvalue: raw p-value; FDR: Benjamini-Hochberg FDR adjusted p-value

Gene Set	NGenes	Direction	PValue	FDR
HALLMARK_INTERFERON_ALPHA_RESPONSE	127	Down	2.60E-07	1.30E-05
HALLMARK_INTERFERON_GAMMA_RESPONSE	217	Down	4.34E-05	0.001

Table 3: Hallmark IFN Alpha Genes 22-25 (3 hpi) versus 22-20 (3 hpi). Genes that contributed to the Hallmark Interferon Alpha Response Gene Set with an adjusted p-value < 0.05. The group comparison is solely 22-25 versus 22-20. ENSEMBL: Ensembl name for gene; SYMBOL: HUGO Gene Nomenclature Committee (HGNC) approved gene symbol; logFC: log fold change; AveExpr: Average expression of the gene across all samples; P.Value: raw p-value; adj.P.Val: Benjamini-Hochberg correction statistic for multiple tests.

ENSEMBL	SYMBOL	logFC	AveExpr	P.Value	adj.P.Val
ENSMUSG00000034855	Cxcl10	-4.03	0.91	1.36E-05	0.012
ENSMUSG00000002325	Irf9	-0.72	3.44	4.94E-05	0.022
ENSMUSG00000074896	Ifit3	-3.10	0.57	7.10E-05	0.022
ENSMUSG00000028270	Gbp2	-5.27	-1.82	2.02E-04	0.038
ENSMUSG00000020641	Rsad2	-6.31	-0.77	4.24E-04	0.049

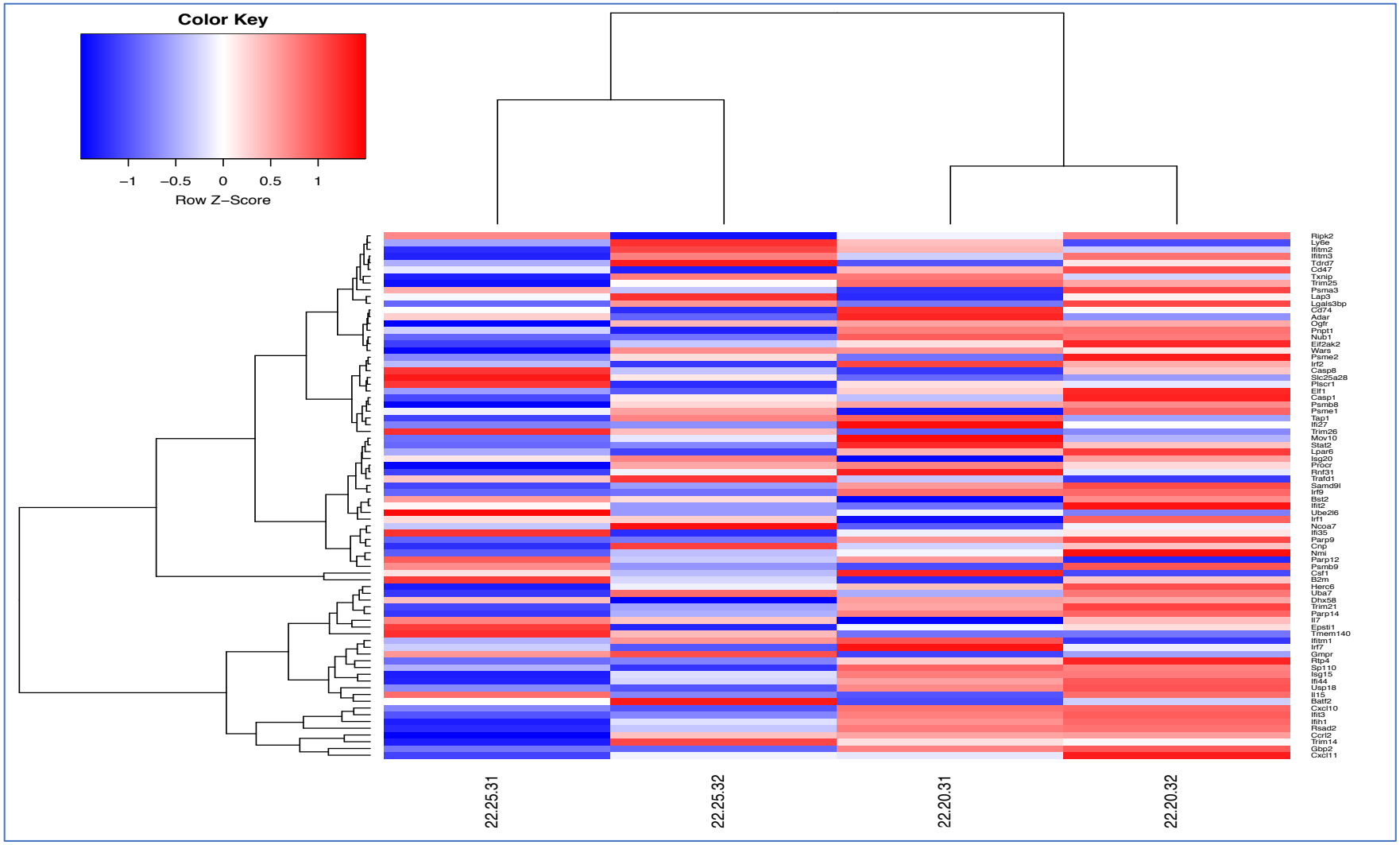

Figure 13. Hallmark Interferon Alpha Response Gene Set. Genes that contributed to the enrichment of this gene set were matched to those the group comparison of 22-25 (3 hpi) and 22-20 (3 hpi). The expression values for these same genes were analyzed across all samples and normalized to standard deviation units (z-score) by row (genes). No adjusted p-value cutoff was used to ensure a more comprehensive model. Gene names are shown along the right side of the heatmap. Red: increased expression, blue: decreased expression. The dendrogram at the top of the heatmap displays the hierarchical clustering of the virus sample replicates. The dendrogram to the left of the heatmap displays the hierarchical clustering of genes, with gene names shown along the right side of the heatmap

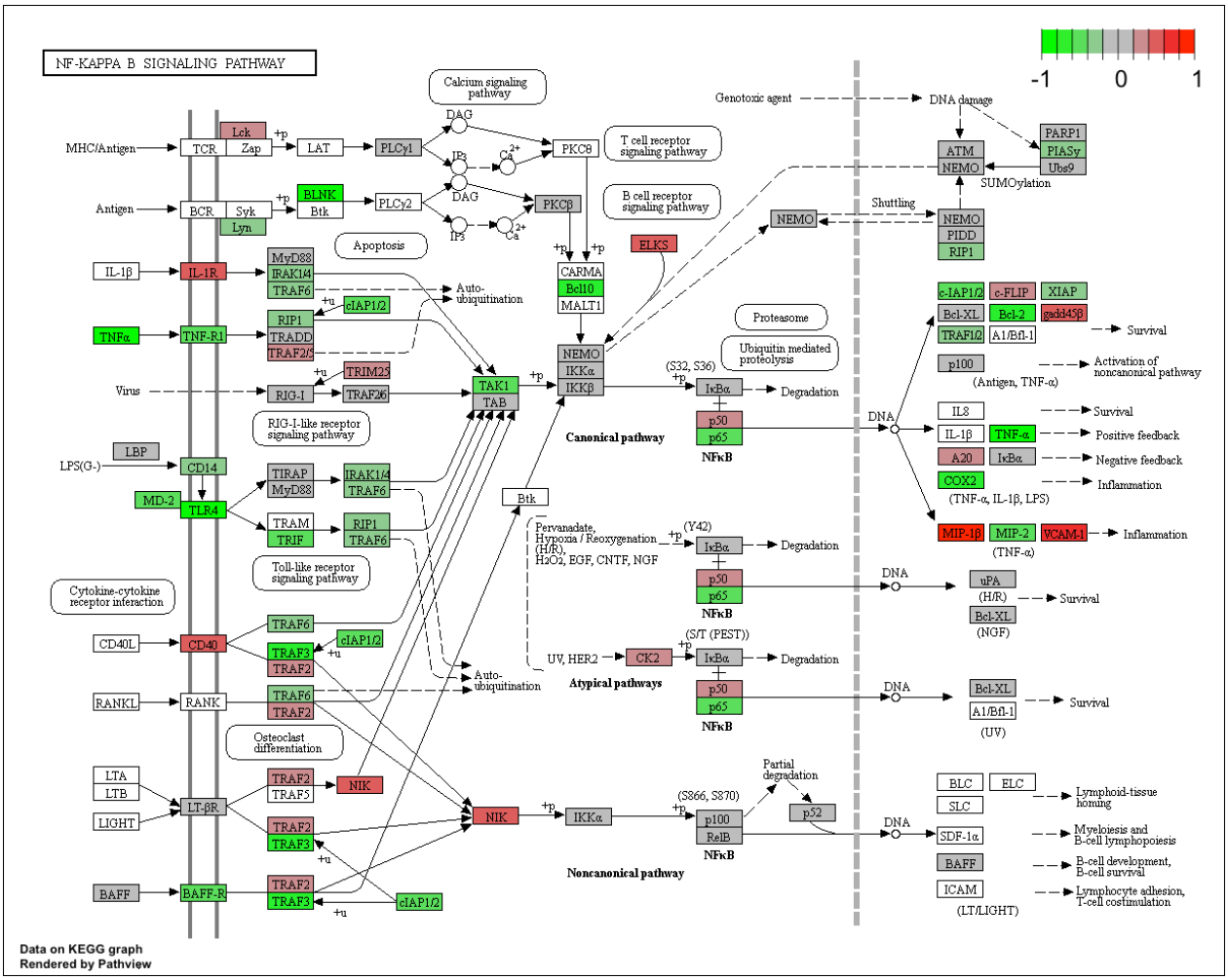

Figure 14. NF-κB Signaling Pathway: 22-20 (3 hpi) versus Mock (3 hpi). Genes involved in NF-κB Signaling Pathway for the group comparison of 22-20 (3 hpi) versus Mock (3 hpi). Key indicates log2 fold-change (lfc). Red: increased expression, green: decreased expression.

Table 4: NF-κB Signaling Pathway - DEGs: 22-20 (3 hpi) versus Mock. Genes involved in the NF-κB Signaling Pathway with an adjusted p-value < 0.05. The group comparison is solely 22-20 (3 hpi) versus Mock. ENSEMBL: Ensembl name for gene; SYMBOL: HGNC approved gene symbol; logFC: log fold change; AveExpr: Average expression of the gene across all samples; P.Value: raw p-value; adj.P.Val: Benjamini-Hochberg correction statistic for multiple tests.

ENSEMBL	SYMBOL	logFC	AveExpr	P.Value	adj.P.Val
ENSMUSG00000061132	Blnk	-1.44	-0.48	5.35E-03	2.73E-02
ENSMUSG00000024401	Tnf	-1.19	1.87	2.38E-05	7.10E-04
ENSMUSG00000021277	Traf3	-0.80	5.65	5.66E-03	2.84E-02
ENSMUSG00000057329	Bcl2	-0.79	4.78	5.88E-05	1.30E-03
ENSMUSG00000028191	Bcl10	-0.71	5.24	2.01E-06	1.56E-04
ENSMUSG00000032487	Ptgs2	-0.71	6.33	3.83E-05	9.60E-04
ENSMUSG00000026875	Traf1	-0.63	3.93	1.84E-03	1.29E-02
ENSMUSG00000047123	Ticam1	-0.52	4.21	4.44E-04	4.80E-03
ENSMUSG00000030341	Tnfrsf1a	-0.47	6.53	2.85E-05	7.99E-04
ENSMUSG00000024927	Rela	-0.42	6.36	1.02E-03	8.51E-03
ENSMUSG00000035476	Tab3	-0.29	4.87	6.99E-03	3.31E-02
ENSMUSG00000027164	Traf6	-0.28	5.76	6.05E-03	2.99E-02
ENSMUSG00000042228	Lyn	-0.27	5.00	1.07E-02	4.43E-02
ENSMUSG00000028163	Nfkb1	0.30	7.33	1.44E-03	1.09E-02
ENSMUSG00000017652	Cd40	0.43	5.03	3.15E-04	3.86E-03
ENSMUSG00000022414	Tab1	0.43	5.34	1.15E-03	9.27E-03
ENSMUSG00000020941	Map3k14	0.54	4.94	7.20E-05	1.46E-03
ENSMUSG00000026072	Il1r1	0.56	6.76	3.57E-03	2.06E-02
ENSMUSG00000015312	Gadd45b	0.59	5.79	3.49E-04	4.11E-03
ENSMUSG00000027962	Vcam1	0.76	6.54	9.08E-07	9.32E-05
ENSMUSG00000018930	Ccl4	5.65	-2.94	1.29E-03	1.01E-02

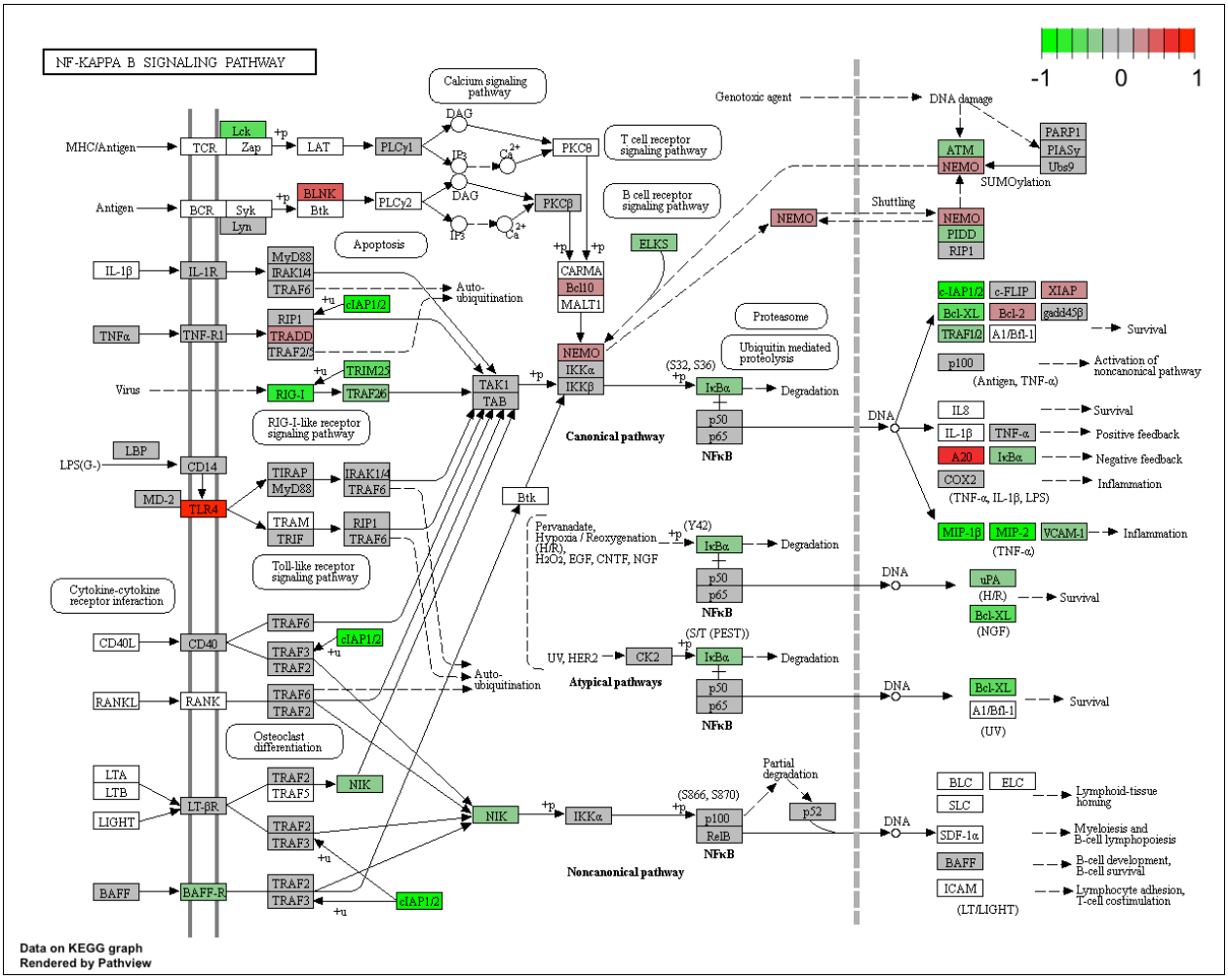

Figure 15. NF-κB Signaling Pathway: 22-25 (3 hpi) versus 22-20 (3 hpi). Genes involved in NF-κB Signaling Pathway for the group comparison of 22-25 (3 hpi) versus 22-20 (3 hpi). Key indicates log2 fold-change. Red: increased expression, green: decreased expression.

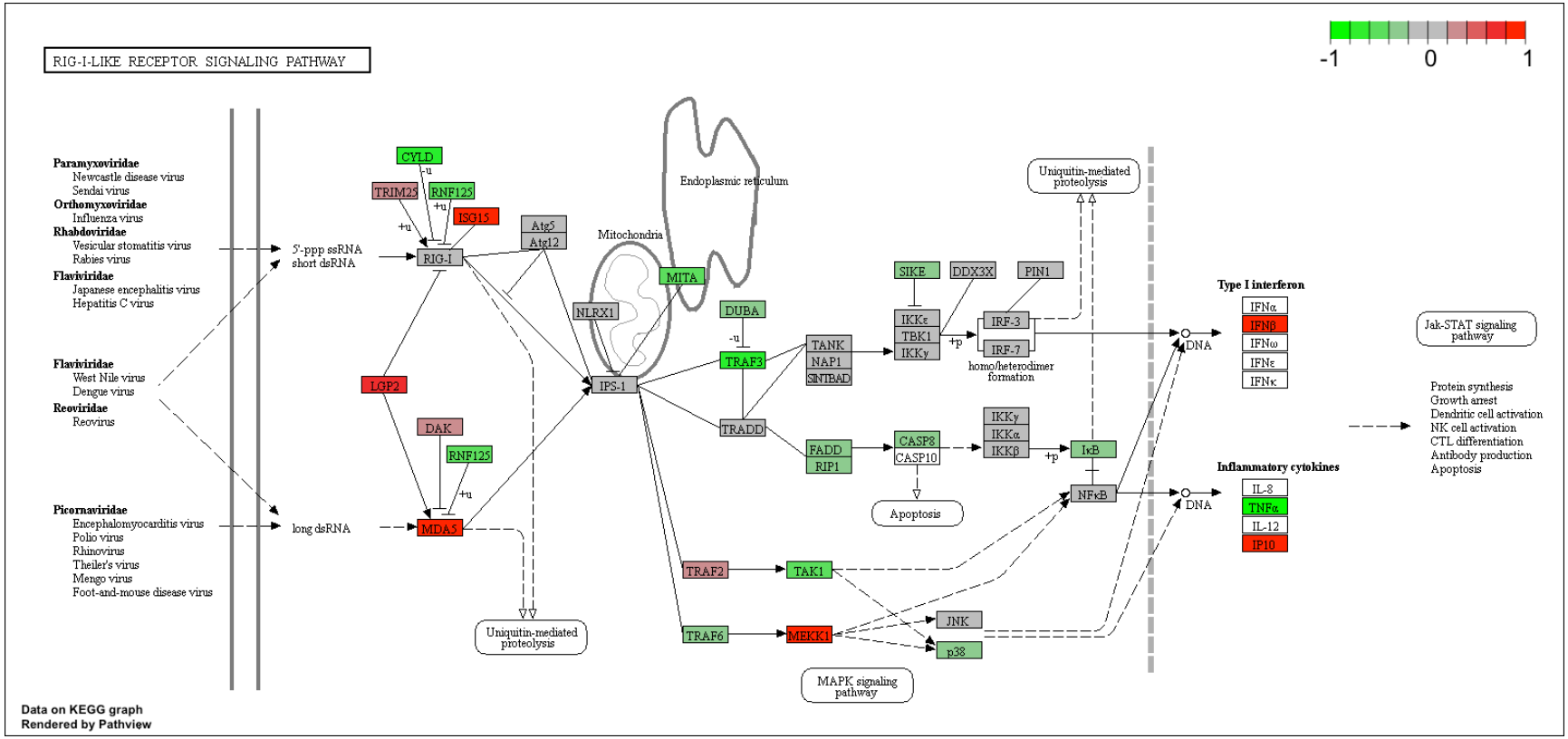

Figure 16. RIG-I Like Receptor Pathway: 22-20 (3 hpi) versus Mock (3 hpi). Genes involved in RIG-I Like Receptor Pathway for the group comparison of 22-20 (3 hpi) versus Mock (3 hpi). Key indicates log2 fold-change. Red: increased expression, green: decreased expression.

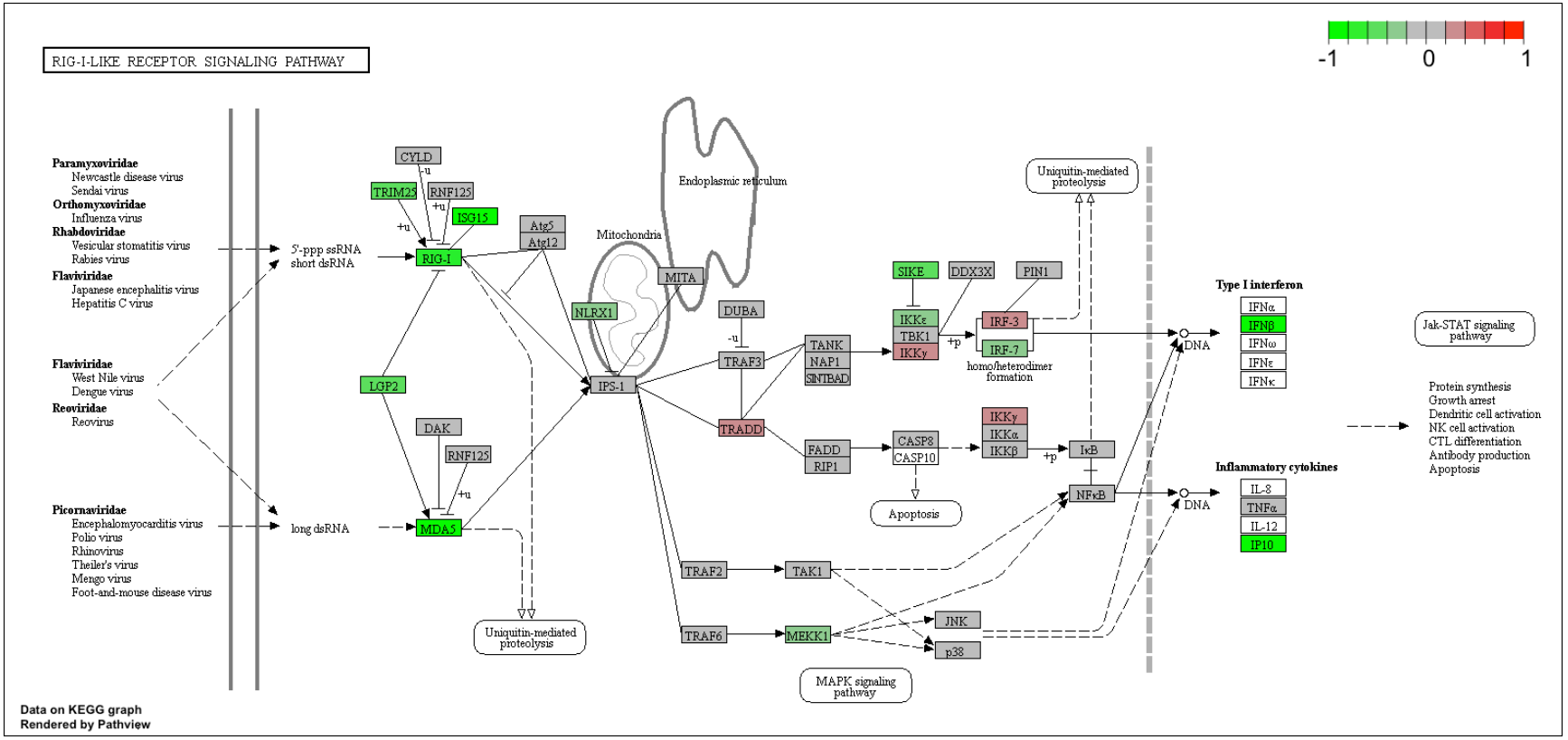

Figure 17. RIG-I Like Receptor Signaling Pathway: 22-25 (3 hpi) versus 22-20 (3 hpi). Genes involved in RIG-I Like Receptor Signaling Pathway for the group comparison of 22-25 (3 hpi) versus 22-20 (3 hpi). Key indicates log2 fold-change. Red: increased expression, green: decreased expression.

Table 5. RIG-I Like Receptor Signaling Pathway DEGs. Genes involved in the RIG-I-Like Signaling Receptor Pathway with an adjusted p-value < 0.05. The first column displays the group comparison within which the genes are expressed. ENSEMBL: Ensembl name for gene; SYMBOL: HGNC approved gene symbol; logFC: log fold change; AveExpr: Average expression of the gene across all samples; P.Value: raw p-value; adj.P.Val: Benjamini-Hochberg correction statistic for multiple tests.

	ENSEMBL	SYMBOL	logFC	AveExpr	P.Value	adj.P.Val
22-20 vs Mock	ENSMUSG00000024401	Tnf	-1.19	1.87	2.38E-05	7.10E-04
22-20 vs Mock	ENSMUSG00000057329	Bcl2	-0.79	4.78	5.88E-05	1.30E-03
22-20 vs Mock	ENSMUSG00000028191	Bcl10	-0.71	5.24	2.01E-06	1.56E-04
22-20 vs Mock	ENSMUSG00000032487	Ptgs2	-0.71	6.33	3.83E-05	9.60E-04
22-20 vs Mock	ENSMUSG00000047123	Ticam1	-0.52	4.21	4.44E-04	4.80E-03
22-20 vs Mock	ENSMUSG00000030341	Tnfrsf1a	-0.47	6.53	2.85E-05	7.99E-04
22-20 vs Mock	ENSMUSG00000017652	Cd40	0.43	5.03	3.15E-04	3.86E-03
22-20 vs Mock	ENSMUSG00000020941	Map3k14	0.54	4.94	7.20E-05	1.46E-03
22-20 vs Mock	ENSMUSG00000015312	Gadd45b	0.59	5.79	3.49E-04	4.11E-03
22-20 vs Mock	ENSMUSG00000027962	Vcam1	0.76	6.54	9.08E-07	9.32E-05
22-25 vs 22-20	ENSMUSG00000034855	Cxcl10	-4.03	0.91	1.36E-05	1.15E-02

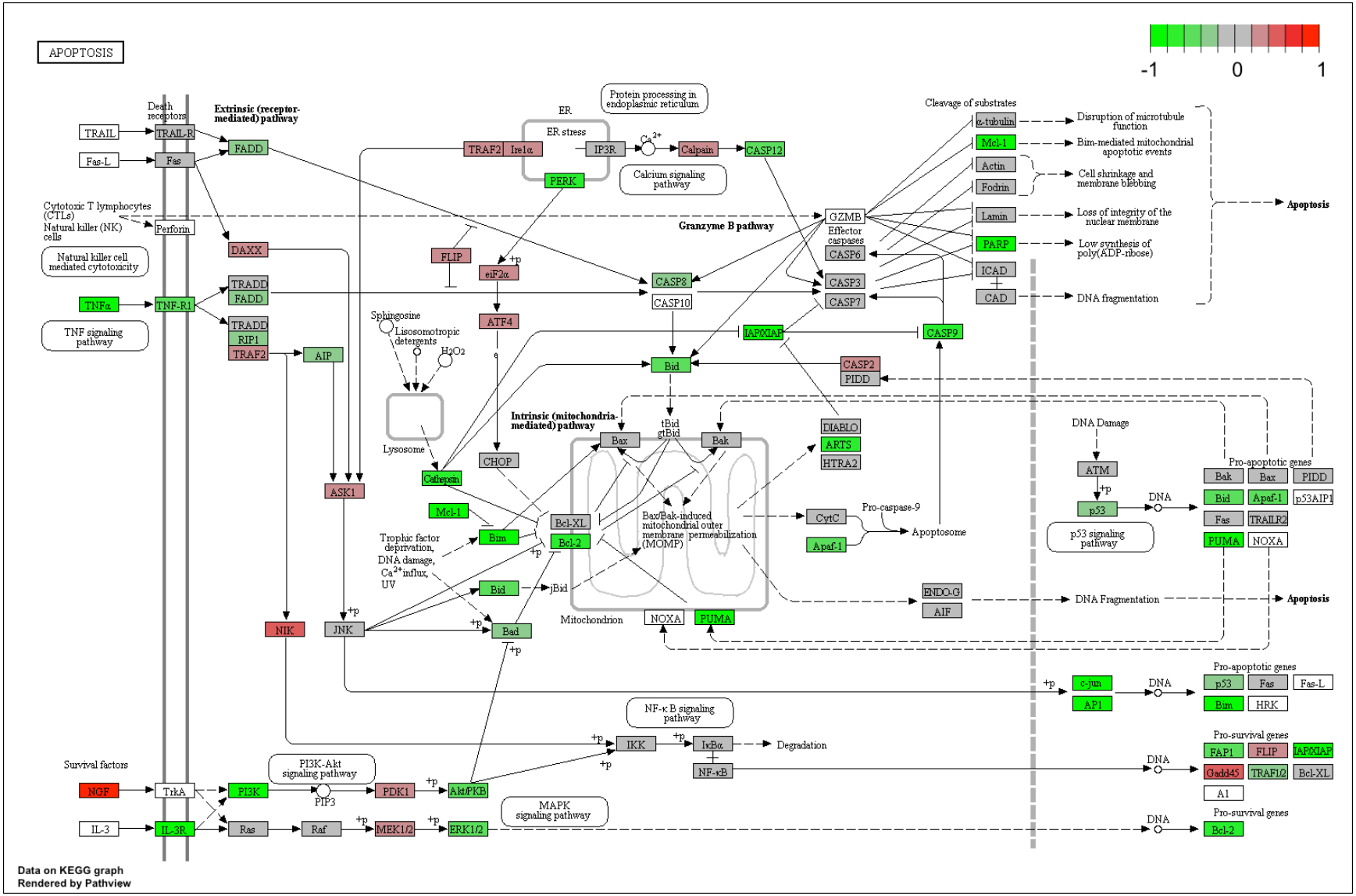

Figure 18. Apoptosis: 22-20 (3 hpi) versus Mock (3 hpi). Genes involved in Apoptosis for the group comparison of 22-20 versus Mock. Key indicates log2 fold-change. Red: increased expression, green: decreased expression.

Table 6. Apoptosis. Genes involved in Apoptosis with an adjusted p-value < 0.05. The first column displays the group comparison within which the genes are expressed. Highlighted gene symbols indicate genes that were expressed differently within multiple group comparisons. ENSEMBL: Ensembl name for gene; SYMBOL: HGNC approved gene symbol; logFC: log fold change; AveExpr: Average expression of the gene across all samples; P.Value: raw p-value; adj.P.Val: Benjamini-Hochberg correction statistic for multiple tests.

	ENSEMBL	SYMBOL	logFC	AveExpr	P.Value	adj.P.Val
22-20 vs Mock	ENSMUSG00000021250	Fos	-6.27	3.12	2.08E-10	3.24E-07
22-20 vs Mock	ENSMUSG00000039936	Pik3cd	-2.23	-0.16	2.30E-04	3.16E-03
22-20 vs Mock	ENSMUSG00000002083	Bbc3	-2.07	2.24	2.17E-06	1.64E-04
22-20 vs Mock	ENSMUSG00000024401	Tnf	-1.19	1.87	2.38E-05	7.10E-04
22-20 vs Mock	ENSMUSG00000052684	Jun	-1.05	6.55	9.43E-08	2.12E-05
22-20 vs Mock	ENSMUSG00000027381	Bcl2l11	-0.91	5.78	1.75E-05	5.97E-04
22-20 vs Mock	ENSMUSG00000038612	Mcl1	-0.81	8.96	4.08E-07	5.29E-05
22-20 vs Mock	ENSMUSG00000057329	Bcl2	-0.79	4.78	5.88E-05	1.30E-03
22-20 vs Mock	ENSMUSG00000028914	Casp9	-0.75	3.85	2.43E-03	1.57E-02
22-20 vs Mock	ENSMUSG00000026875	Traf1	-0.63	3.93	1.84E-03	1.29E-02
22-20 vs Mock	ENSMUSG00000031668	Eif2ak3	-0.61	5.16	4.99E-05	1.16E-03
22-20 vs Mock	ENSMUSG00000023249	Parp3	-0.58	4.14	3.85E-04	4.35E-03
22-20 vs Mock	ENSMUSG00000004446	Bid	-0.55	6.76	1.36E-05	5.20E-04
22-20 vs Mock	ENSMUSG00000030341	Tnfrsf1a	-0.47	6.53	2.85E-05	7.99E-04
22-20 vs Mock	ENSMUSG00000025887	Casp12	-0.45	4.64	1.01E-03	8.47E-03
22-20 vs Mock	ENSMUSG00000019979	Apaf1	-0.45	4.80	4.53E-03	2.43E-02
22-20 vs Mock	ENSMUSG00000024927	Rela	-0.42	6.36	1.02E-03	8.51E-03
22-20 vs Mock	ENSMUSG00000034573	Ptpn13	-0.42	4.75	2.94E-03	1.79E-02
22-20 vs Mock	ENSMUSG00000054509	Parp4	-0.42	4.61	7.99E-03	3.62E-02
22-20 vs Mock	ENSMUSG00000024959	Bad	-0.37	4.61	1.16E-02	4.71E-02
22-20 vs Mock	ENSMUSG00000059552	Trp53	-0.36	6.84	1.17E-02	4.73E-02
22-20 vs Mock	ENSMUSG00000031834	Pik3r2	-0.34	6.81	1.82E-04	2.67E-03
22-20 vs Mock	ENSMUSG00000024590	Lmnb1	-0.29	7.34	1.53E-03	1.14E-02
22-20 vs Mock	ENSMUSG00000063065	Mapk3	-0.24	6.45	1.08E-02	4.47E-02

22-20 vs Mock	ENSMUSG00000023004	Tuba1b	0.20	9.87	9.90E-03	4.20E-02
22-20 vs Mock	ENSMUSG00000042406	Atf4	0.24	8.73	1.60E-03	1.17E-02
22-20 vs Mock	ENSMUSG00000026509	Capn2	0.26	8.08	9.56E-04	8.18E-03
22-20 vs Mock	ENSMUSG00000028163	Nfkb1	0.30	7.33	1.44E-03	1.09E-02
22-20 vs Mock	ENSMUSG00000071369	Map3k5	0.32	5.71	8.15E-04	7.30E-03
22-20 vs Mock	ENSMUSG00000041417	Pik3r1	0.35	6.78	7.31E-04	6.82E-03
22-20 vs Mock	ENSMUSG00000004936	Map2k1	0.36	6.09	1.29E-04	2.11E-03
22-20 vs Mock	ENSMUSG00000028063	Lmna	0.36	9.95	4.08E-03	2.26E-02
22-20 vs Mock	ENSMUSG00000024122	Pdpk1	0.37	6.94	7.94E-04	7.17E-03
22-20 vs Mock	ENSMUSG00000020941	Map3k14	0.54	4.94	7.20E-05	1.46E-03
22-20 vs Mock	ENSMUSG00000015312	Gadd45b	0.59	5.79	3.49E-04	4.11E-03
22-20 vs Mock	ENSMUSG00000027859	Ngf	1.01	6.59	1.59E-04	2.45E-03
22-25 vs 22-20	ENSMUSG00000042406	Atf4	0.36	8.73	9.61E-05	2.49E-02
22-25 vs 22-20	ENSMUSG00000030265	Kras	0.45	6.33	1.16E-04	2.77E-02
22-25 vs 22-20	ENSMUSG00000038612	Mcl1	0.50	8.96	1.80E-05	1.33E-02

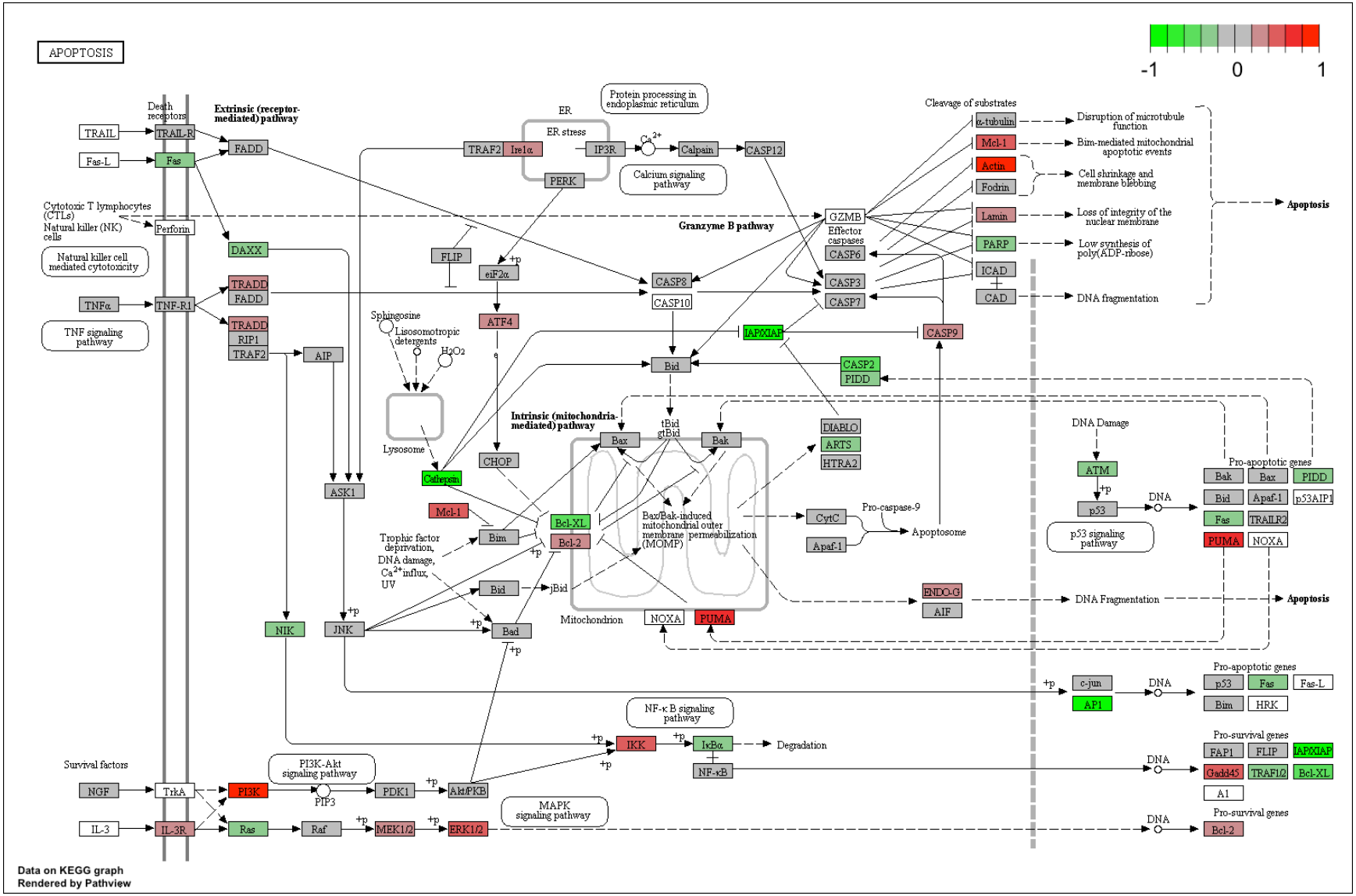

Figure 19. Apoptosis: 22-25 (3 hpi) versus 22-20 (3 hpi). Genes involved in Apoptosis for the group comparison of 22-25 (3 hpi) versus 22-20 (3 hpi). Key indicates log fold-change. Red: increased expression, green: decreased expression.

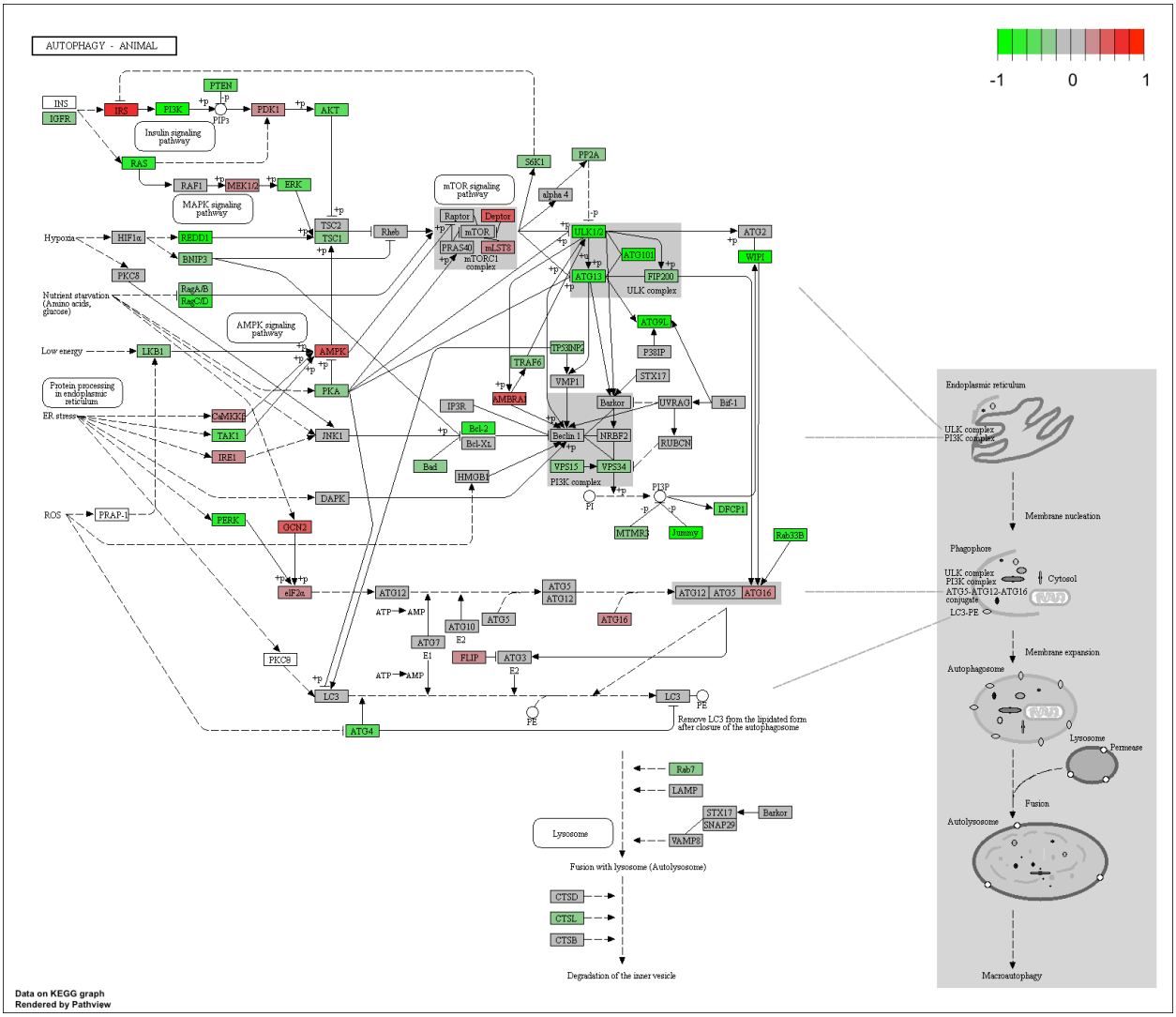

Figure 20. Autophagy - Animal: 22-20 (3 hpi) versus Mock (3 hpi). Genes involved in Autophagy – Animal for the group comparison of 22-20 (3 hpi) versus Mock (3 hpi). Key indicates log fold-change. Red: increased expression, green: decreased expression.

Table 7. Autophagy. Genes involved in Autophagy with an adjusted p-value < 0.05. The first column displays the group comparison within which the genes are expressed. ENSEMBL: Ensembl name for gene; SYMBOL: HGNC approved gene symbol; logFC: log fold change; AveExpr: Average expression of the gene across all samples; P.Value: raw p-value; adj.P.Val: Benjamini-Hochberg correction statistic for multiple tests.

	ENSEMBL	SYMBOL	logFC	AveExpr	P.Value	adj.P.Val
22-20 vs Mock	ENSMUSG00000039936	Pik3cd	-2.23	-0.16	2.30E-04	3.16E-03
22-20 vs Mock	ENSMUSG00000020108	Ddit4	-1.21	4.77	1.82E-06	1.46E-04
22-20 vs Mock	ENSMUSG00000037204	Atg101	-1.16	4.16	2.06E-05	6.48E-04
22-20 vs Mock	ENSMUSG00000030269	Mtmr14	-1.05	3.64	1.03E-05	4.43E-04
22-20 vs Mock	ENSMUSG00000038894	Irs2	-0.91	7.40	2.27E-07	3.80E-05
22-20 vs Mock	ENSMUSG00000057329	Bcl2	-0.79	4.78	5.88E-05	1.30E-03
22-20 vs Mock	ENSMUSG00000033124	Atg9a	-0.66	5.13	6.67E-04	6.43E-03
22-20 vs Mock	ENSMUSG00000041895	Wipi1	-0.64	4.79	6.52E-05	1.38E-03
22-20 vs Mock	ENSMUSG00000029512	Ulk1	-0.64	4.32	9.08E-05	1.68E-03
22-20 vs Mock	ENSMUSG00000027244	Atg13	-0.64	4.49	1.84E-04	2.69E-03
22-20 vs Mock	ENSMUSG00000028550	Atg4c	-0.63	2.38	5.63E-03	2.83E-02
22-20 vs Mock	ENSMUSG00000031668	Eif2ak3	-0.61	5.16	4.99E-05	1.16E-03
22-20 vs Mock	ENSMUSG00000042628	Zfyve1	-0.59	3.54	2.63E-03	1.66E-02
22-20 vs Mock	ENSMUSG00000013663	Pten	-0.51	7.12	2.76E-05	7.85E-04
22-20 vs Mock	ENSMUSG00000028278	Rragd	-0.44	3.72	1.92E-03	1.33E-02
22-20 vs Mock	ENSMUSG00000078566	Bnip3	-0.39	4.53	8.83E-03	3.88E-02
22-20 vs Mock	ENSMUSG00000024959	Bad	-0.37	4.61	1.16E-02	4.71E-02
22-20 vs Mock	ENSMUSG00000025907	Rb1cc1	-0.36	4.46	3.79E-03	2.15E-02
22-20 vs Mock	ENSMUSG00000032470	Mras	-0.36	4.10	4.48E-03	2.41E-02
22-20 vs Mock	ENSMUSG00000031834	Pik3r2	-0.34	6.81	1.82E-04	2.67E-03
22-20 vs Mock	ENSMUSG00000038375	Trp53inp2	-0.32	6.50	1.68E-03	1.21E-02
22-20 vs Mock	ENSMUSG00000033628	Pik3c3	-0.31	4.29	7.16E-03	3.37E-02
22-20 vs Mock	ENSMUSG00000070934	Rraga	-0.29	6.74	6.75E-04	6.49E-03
22-20 vs Mock	ENSMUSG00000027164	Traf6	-0.28	5.76	6.05E-03	2.99E-02
22-20 vs Mock	ENSMUSG00000063065	Mapk3	-0.24	6.45	1.08E-02	4.47E-02
22-20 vs Mock	ENSMUSG00000029578	Wipi2	-0.23	7.74	3.73E-03	2.13E-02
22-20 vs Mock	ENSMUSG00000029471	Camkk2	0.32	6.59	1.17E-02	4.73E-02

22-20 vs Mock	ENSMUSG00000041417	Pik3r1	0.35	6.78	7.31E-04	6.82E-03
22-20 vs Mock	ENSMUSG00000004936	Map2k1	0.36	6.09	1.29E-04	2.11E-03
22-20 vs Mock	ENSMUSG00000024122	Pdpk1	0.37	6.94	7.94E-04	7.17E-03
22-20 vs Mock	ENSMUSG00000024142	Mlst8	0.39	5.22	1.10E-03	9.01E-03
22-20 vs Mock	ENSMUSG00000026289	Atg16l1	0.41	5.85	8.11E-04	7.27E-03
22-20 vs Mock	ENSMUSG00000040506	Ambra1	0.41	5.32	4.14E-03	2.28E-02
22-20 vs Mock	ENSMUSG00000022419	Deptor	0.45	6.11	1.62E-03	1.18E-02
22-20 vs Mock	ENSMUSG00000005102	Eif2ak4	0.51	5.54	8.31E-04	7.39E-03
22-20 vs Mock	ENSMUSG00000041341	Atg2b	0.51	5.65	2.86E-03	1.76E-02
22-20 vs Mock	ENSMUSG00000055980	Irs1	1.63	8.36	6.77E-08	1.65E-05
25-20 vs 22-20	ENSMUSG00000030265	Kras	0.45	6.33	0.0001	0.03

Finally, 37 genes in the Autophagy pathway were found to be differentially expressed (FDR < 0.05) in 22-20 (3hpi) versus Mock (1hpi) with 11 upregulated and 26 downregulated (Table 7). One gene, Kras, was found to be downregulated in 22-25 (3hpi) versus 22-20 (3hpi). It seems, therefore, at that the D52G mutation does not have a significant effect on these pathways at the transcription level, since there are very few significantly different genes between the 22-25 and 22-20 groups. However, these small variations on certain genes may reveal what changes have occurred in the host due to the D52G mutation in the M protein.

Gene Ontology (GO) analysis demonstrates the effect of the 22-20 and 22-25 viruses on separate groups of genes. Biological processes involved with host response to virus were upregulated in 22-20 when compared to Mock, and there appears to be no further upregulation by 22-25 for the same groups when compared to 22-20 (Figure 22). This is to be expected, as the host cell would begin to defend itself in the initial stages of infection. However, 22-25 is has a greater level of downregulated genes that are involved in the biological processes for viral

response (Figure 23). This indicates that while earlier analysis showed there were few genes of significant difference within certain pathways, overall immune response to 22-25 is reduced in comparison to 22-20. Furthermore, though 22-25 continues to down regulate other biological processes in comparison to 22-20, including RNA metabolism and cell death, the overwhelming differences between the two viruses are within the viral response processes.

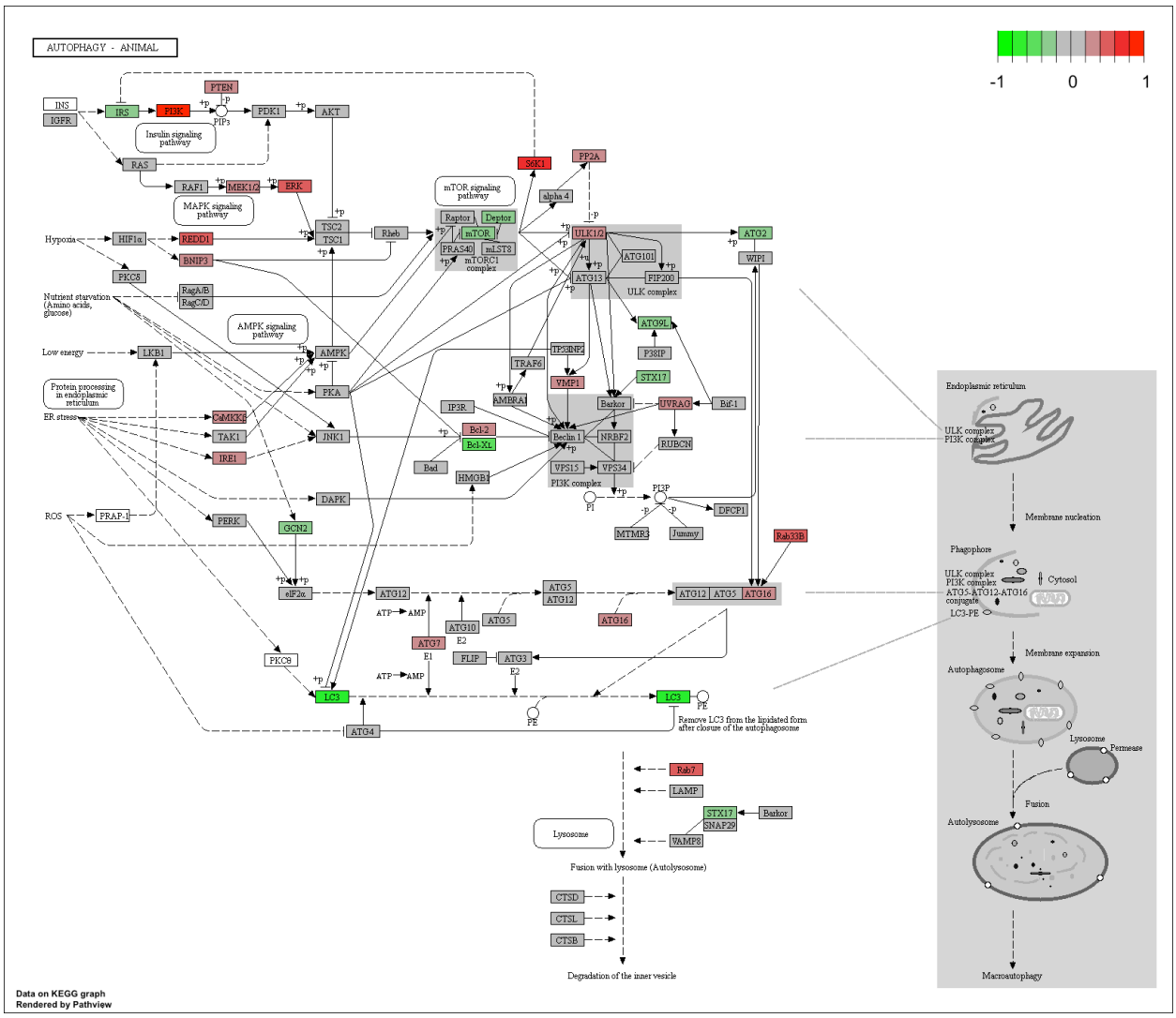

Figure 21. Autophagy - Animal: 22-25 (3 hpi) versus 22-20 (3 hpi). Genes involved in Autophagy – Animal for the group comparison of 22-25 (3 hpi) versus 22-20 (3 hpi). Key indicates log fold-change. Red: increased expression, green: decreased expression.

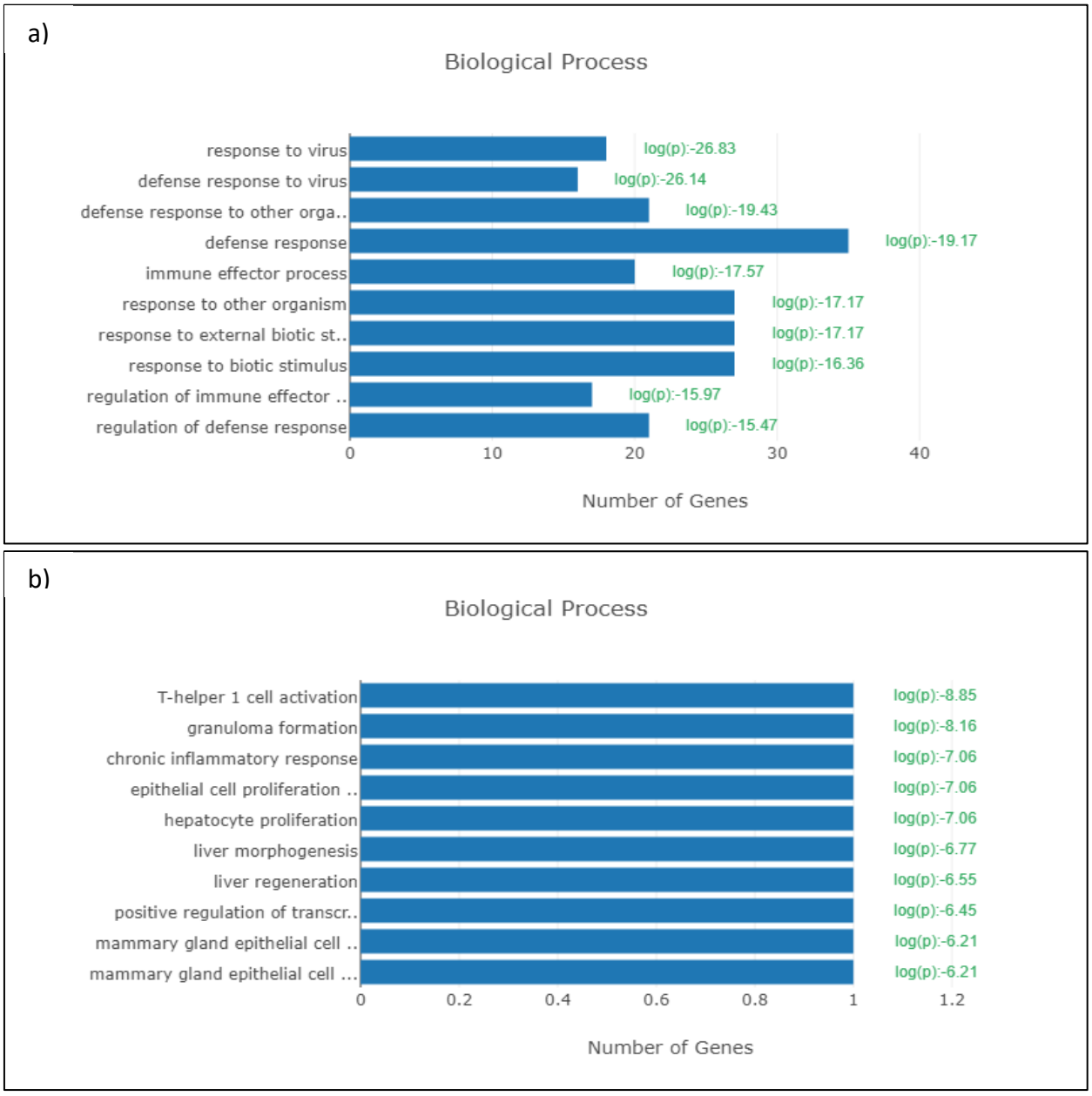

Figure 22. Biological Process: Up Regulated Genes. These biological processes from the Gene Ontology (GO) were found to be enriched through Gene Set Enrichment Analysis (GSEA). a) 22-20-3 versus Mock (3 hpi), Processes: response to virus, defense response to virus, defense response to other organisms, defense response, immune effector process, response to other organism, response to external biotic stimulus, response to biotic stimulus, regulation of immune effector process, regulation of defense response; b) 22-25 (3 hpi) versus 22-20 (3 hpi), Processes: T-helper 1 cell activation, granuloma formation, chronic inflammatory response, chronic inflammatory response, epithelial cell proliferation involved in liver morphogenesis, hepatocyte proliferation, liver morphogenesis, liver regeneration, positive regulation of transcription from RNA polymerase II promoter in response to endoplasmic reticulum stress, mammary gland epithelial cell differentiation, mammary gland epithelial cell proliferation.

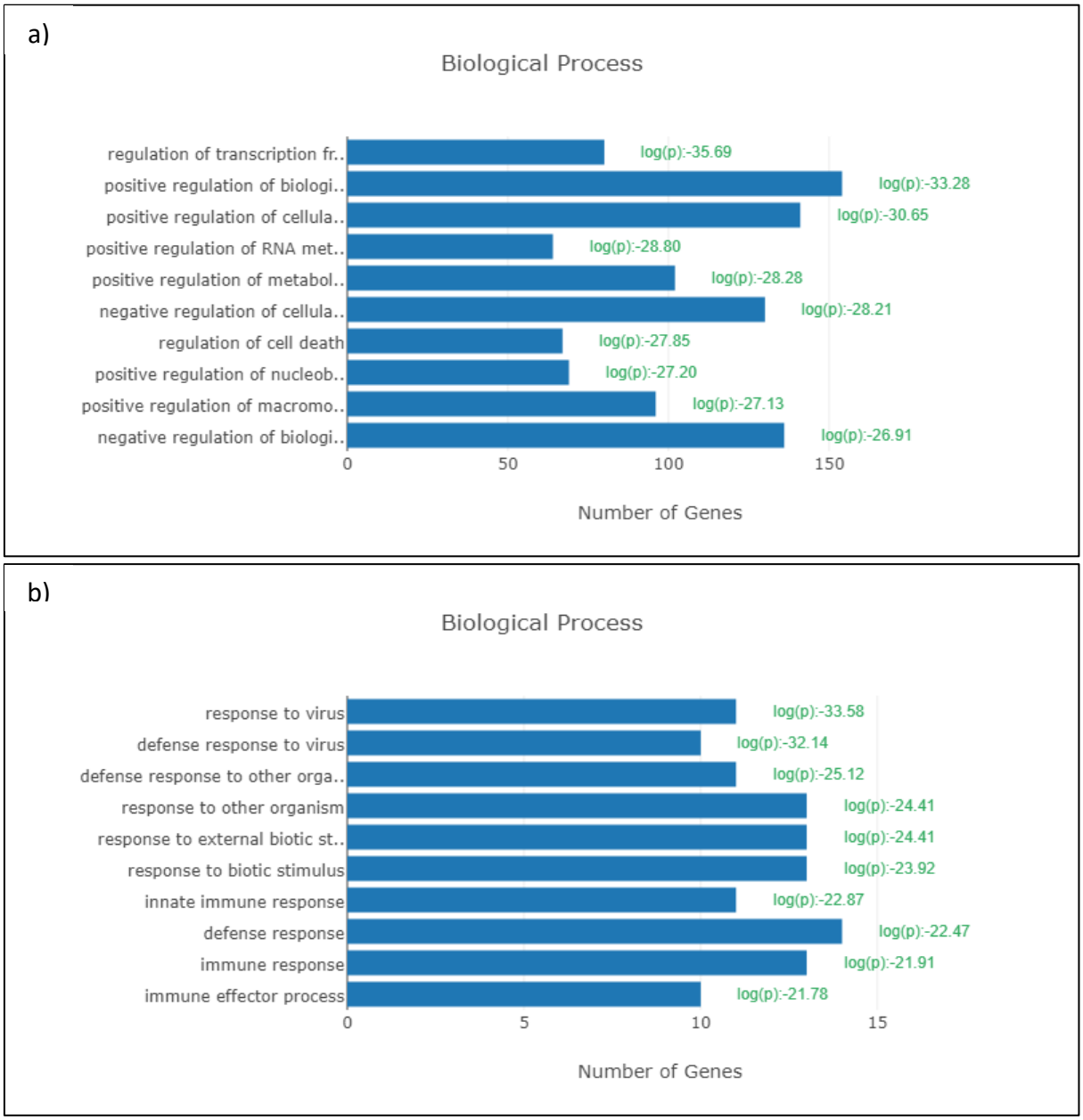

Figure 23. Biological Process: Down Regulated Genes. These biological processes from the Gene Ontology (GO) were found to be enriched through Gene Set Enrichment Analysis (GSEA). a) 22-20-3 versus Mock (3 hpi), Processes: regulation of transcription from RNA polymerase II promoter, positive regulation of biological process, positive regulation of cellular process, positive regulation of RNA metabolic process, positive regulation of metabolic process, negative regulation of cellular process, regulation of cell death, positive regulation of nucleobase-containing compound metabolic process, positive regulation of macromolecule metabolic process, negative regulation of biological process; b) 22-25 (3 hpi) versus 22-20 (3 hpi), Processes: response to virus, defense response to virus, defense response to other organism, response to other organism, response to external biotic stimulus, response to biotic stimulus, innate immune response , defense response, immune response , immune effector process.

Discussion

Until recently, it was believed that the 22-20 and 22-25 M protein gene sequences were identical (14), however we identified a D52G mutation in the M protein of 22-20 (unpublished), which abrogates its ability to inhibit NF-κB. We also found that little to no IFN mRNA or protein in 22-20 infected L929 cells, which we propose was due to M-mediated inhibition of host transcription. With this in mind the goals of this study were the following: (1) find NF-κB response genes that are differentially expressed between 22-25 and 22-20, (2) determine host pathways that are affected by the M protein, and (3) identify host genes that may be involved in M-mediated inhibition of host transcription and/or regulation of the IFN response.

First, the results of the MDS plot indicate that our VSV mutants elicit unique host gene responses, while still conveying important clustering results. That fact that mock and 22-20 (1hpi) cluster together, illustrates that one hour is not a sufficient time lapse to see meaningful changes in host transcription. Conversely, the correlation between wt (3hpi) and 22-20 (3hpi), indicates that the host response to these mutants is similar. Overall, it can be determined that our samples should provide us with reliable data.

The clustering of different samples and biological groups (Figure 6) was confirmed through hierarchical clustering and heatmap analysis of genes which suggests that 22-20 and wt have a similar impact on overall host gene expression, even though they are discordant for NF-κB activation (12). We expected that wt and 22-25 would cluster since their M proteins do not contain M51R or D52G mutations, they both block NF-κB activation, and they both inhibit host

transcription (Table 1). It is possible that wt clusters closely to the 22-20 mutant because wt is a "lab strain" virus and therefore, wt may be attenuated in comparison to 22-25.

We also determined that there were no DEGs between 22-25 and 22-20 for the NF-κB pathway, suggesting that these viruses do no target molecules in this pathway at the transcriptional level. Therefore, we hypothesize that these viruses regulate the function of one of the proteins in this pathway by altering its translation, stability, or PTM such as phosphorylation or ubiquitination. In fact, a recent study found that VSV encoding the M(M51R) mutation did exert distinct changes at the proteome and phosphoproteome levels compared to mock-infected cells (36). In contrast, we see only a few genes that are significantly differentially expressed between 22-25 and 22-20 at 3hpi on the transcriptomic level. This may be due to the fact that 22-20 and 22-25 both inhibit overall host transcription, rendering most differences in gene expression insignificant. The evasion of the innate immune response via PTM would not be unique to VSV. Many viruses, including Influenza A, Hepatitis B, and Ebola, have developed mechanism by which they circumvent the immune response (37). Therefore, we believe viruses such as R1 and 22-20 may activate positive regulators of the NF-kB pathway by effecting the proteome or PTM of key components, resulting in NF-kB activation. These viruses may also inactivate negative regulators of the pathway. In contrast viruses that are able to block NF-kB (wt, 22-25) may inactivate positive regulators, or activate negative regulators of this pathway at the protein or PTM level.

The patterns of minimal differences between 22-20 and 22-25, at the transcriptomic level, extended to other important pathways including the RIG-I and autophagy pathways. We found that apoptosis is the only pathway where 22-25 shows significant differences (both up and

downregulated) in genes that are differentially expressed by 22-20. Again, we notice that there is minimal significance at the transcriptional level. However, these significant genes might provide insight into the effect of the M protein on apoptosis. Previous studies have shown that the M protein induces cell rounding, a hallmark of apoptosis and it has been shown that the M protein has an effect on programmed cell death (38). VSV containing an M protein mutant, rM51R-M, illustrated how changes to the M protein affects the pathways through which VSV induces apoptosis (39). The wt virus primarily activated apoptosis through the mitochondrial (intrinsic) pathway via caspase 9 (Casp9), while rM51R-M, primarily activated apoptosis through the death receptor (extrinsic) pathway via caspase 8 (Casp8). It was also observed that rM51R-M induced apoptosis much more rapidly than the wt virus (39). Further research determined the effects of VSV wt on other specific genes within the apoptosis pathway including Mcl1 and Bid (40).

Mcl1 is an antiapoptotic protein within the Bcl2 protein family, which includes both pro and antiapoptotic proteins (40). Mcl1 has a high turnover rate (~1hr) and it was discovered that the wt virus, through its inhibition of host transcription, caused a rapid depletion of the remaining Mcl1 proteins (40). We found that host expression of Mcl1 was more downregulated by 22-20 than by 22-25. This could potentially mean that 22-20 is more effective at overall host gene inhibition than 22-25. However, this is one of the few differences between 22-20 and 22-25 DEGS, so further study is necessary. We also found that Bid, Bcl2 and Casp9 were all downregulated by 22-20 and 22-25. Bid is a proapoptotic member of the Bcl2 family, which is known to instigate cross talk between the extrinsic and intrinsic pathways through activation by Casp8 (40). Casp8 was not found to be differentially expressed by the host in response to 22-20

or 22-25 while the downregulation Bid is likely also due to the inhibition of overall host transcription. The downregulation of Bcl2, found on the mitochondria, might indicate that 22-20 and 22-25 are activating the intrinsic pathway. This would be interesting since rM51R-M primarily activates apoptosis via the extrinsic pathway. Proteomic research could help to determine which pathway is being regulated by 22-20 and 22-25.

We also found that 87 of the same genes are differentially expressed in 22-25 and wt viruses (Figure 12). Since it was discovered that host transcription, in response to 22-25 and wt, do not cluster closely at 3hpi (Figure 6), this group of genes could potentially reveal genes that are important for VSV infection. Two interesting genes, Ifit3 and Rsad2, were both found to be significantly downregulated by 22-25 in comparison to the 22-20 response. The Ifit gene family consists of antiviral factors that are important to the IFN response pathway (41). Ifit3 has been shown to positively regulate the functions of Ifit1, a foreign RNA binding protein. By forming a multiprotein complex with Ifit1, Ifit3 enables are more effective immune response (42). Thus, the downregulation of Ifit3 would negatively affect the ability of Ifit1 to bind to VSV transcription products, which would then hinder the host ability to fight infection. Rsad2, also known as Viperin, is an ISG, which is activated by Type I and II IFN. Many viruses stimulate this protein following their detection by RLRs, however, it has been found that VSV elicits a response by independent means (43, 44). VSV activates IRF1/3 directly, which then stimulates Viperin, effectively circumventing the RLR mediated response (44). Unfortunately, due to the broad activity of Viperin to many viruses, it has been difficult to determine its function in response to VSV. Viperin activities, including metabolism and signaling mediation, tend to be associated with the regulation of lipids (44). This regulation affects Hepatitis C replication and

Influenza budding, there is no known involvement with VSV replication (44). It is therefore possible that the reduced expression of Viperin (and Ifit3) could be due to other factors including overall host transcription inhibition, or the fact that 22-25 has a greater impact on immune response pathways (Figure 23b), or more specifically or 22-20 may be regulating IRF-3 differently than 22-25.

Finally, our GO analysis (Figures 22-23) indicated that when compared to mock, 22-20 downregulated biological processes associated with normal cell function and transcript regulation (Figure 23a). Since we do not see the same gene sets named for 22-25 compared to 22-20 (Figure 23b), we can safely assume that 22-25 is affecting normal function and transcript regulation in a similar manner to 22-20. This suggests that both 22-20 and 22-25 downregulate overall host transcription. As expected, we found that many gene sets associated with infection and the immune response were upregulated by 22-20 (Figure 22a). Host response to 22-25 displays downregulation of biological processes (Figure 23b) that are associated with infection and immune response. It is also worth noting that we did not find any biological processes that were further upregulated by 22-25 in comparison to 22-20 (Figure 22b). These results indicate that 22-25 is more effective at abrogating the immune response, and the two viruses act similarly in terms of down regulating overall transcription. These findings support the heatmaps clustering (Figures 7-9), which indicates the virus samples at 3 hpi downregulate host genes in comparison to 1 hpi samples.

Future Work

There are several interesting projects that we believe could stem from this research. For example, we found that there were 19 DEGs between 22-20 and wt. Further analysis of the pathways affected by these genes and their significance could provide us with insight into the usefulness of 22-20 as an oncolytic agent. As such, since apoptosis activity is an important factor in oncolytics, we could investigate the regulation of apoptosis in 22-20-infected cells. Focusing on specific DEGs that we discovered, we might also investigate the role of Rsad2/Viperin in VSV infection as well as determine whether Ifit3 regulation is affecting Ifit1 activity. We could also perform RNA-Seq analysis on the host transcriptome in response to R1 and compare this response to that of 22-20. This would help to solidify our understanding of the M51R and D52G mutations and their effect on M protein function.

Conclusion

Clinical applications of VSV would benefit tremendously from an improved understanding of VSV-host interactions; therefore, we investigated the effect of VSV on host gene expression. Our findings show that the VSV M protein effects key biological pathways such as RIG-I/NF-κB, IFN-alpha and apoptosis. GO analysis also illustrates how 22-20 and 22-25 affect normal function and transcript regulation similarly, supporting the conclusion that 22-20 and 22-25 both downregulate overall host response. Since 22-20 downregulates host transcription and suppresses the IFN response, it could potentially be an oncolytic viral candidate. There is still, of course, a need to investigate the effect of these viruses on the host at the proteomic level since we found little significant difference between 22-20 and 22-25 at the transcriptomic level for

key pathways. However, evidence that 22-20 downregulates Mcl1 more than 22-25, indicates that 22-20 has potential as an apoptosis promoting viral mutant. By shedding light on how VSV affects the host, these types of studies facilitate the development of VSV as an oncolytic agent and a recombinant vaccine platform.

References

1. Zeng W, Sun L, Jiang X, Chen X, Hou F, Adhikari A, Xu M, Chen ZJ. 2010. Reconstitution of the RIG-I pathway reveals a signaling role of unanchored polyubiquitin chains in innate immunity. Cell 141:315-30.
2. Haller O, Kochs G, Weber F. 2006. The interferon response circuit: induction and suppression by pathogenic viruses. Virology 344:119-30.
3. Wagner RR, Rose JK. 1996. Rhabdoviridae: The Viruses and Their Replication, Third ed. Lipincott - Raven Publishers, Philadelphia.
4. Hinzman EE, Barr JN, Wertz GW. 2008. Selection for gene junction sequences important for VSV transcription. Virology 380:379-87.
5. Finkelshtein D, Werman A, Novick D, Barak S, Rubinstein M. 2013. LDL receptor and its family members serve as the cellular receptors for vesicular stomatitis virus. Proceedings of the National Academy of Sciences of the United States of America 110:7306-7311.
6. Pfaller CK, Cattaneo R, Schnell MJ. 2015. Reverse genetics of Mononegavirales: How they work, new vaccines, and new cancer therapeutics. Virology 479-480:331-44.
7. Faul EJ, Lyles DS, Schnell MJ. 2009. Interferon Response and Viral Evasion by Members of the Family Rhabdoviridae, p 832-51, Viruses, vol 1.
8. Perry AK, Chen G, Zheng D, Tang H, Cheng G. 2005. The host type I interferon response to viral and bacterial infections. Cell Research 15:407-422.
9. Delneste Y, Beauvillain C, Jeannin P. 2007. Immunité naturelle. Med Sci (Paris) 23:67-74.
10. Kato H, Takeuchi O, Sato S, Yoneyama M, Yamamoto M, Matsui K, Uematsu S, Jung A, Kawai T, Ishii KJ, Yamaguchi O, Otsu K, Tsujimura T, Koh CS, Reis e Sousa C, Matsuura Y, Fujita T, Akira S. 2006. Differential roles of MDA5 and RIG-I helicases in the recognition of RNA viruses. Nature 441:101-5.
11. Liu Y, Olagnier D, Lin R. 2016. Host and Viral Modulation of RIG-I-Mediated Antiviral Immunity. Front Immunol 7:662.
12. Varble AJ, Ried CD, Hammond WJ, Marquis KA, Woodruff MC, Ferran MC. 2016. The vesicular stomatitis virus matrix protein inhibits NF-κB activation in mouse L929 cells. Virology 499:99-104.
13. Krug RM. 2014. Viral Proteins That Bind Double-Stranded RNA: Countermeasures Against Host Antiviral Responses, p 464-8, J Interferon Cytokine Res, vol 34.
14. Marcus PI, Sekellick MJ, Spiropoulou CF, Nichol ST. 1993. Interferon induction by viruses. XXII. Vesicular stomatitis virus-Indiana: M-protein and leader RNA do not regulate interferon induction in chicken embryo cells. J Interferon Res 13:413-8.

15. Desforges M, Charron J, Bérard S, Beausoleil S, Stojdl DF, Despars G, Laverdière B, Bell JC, Talbot PJ, Stanners CP, Poliquin L. 2001. Different host-cell shutoff strategies related to the matrix protein lead to persistence of vesicular stomatitis virus mutants on fibroblast cells. Virus Research 76:87-102.
16. Anonymous. 2017. StringTie. http://ccb.jhu.edu/software/stringtie/index.shtml?t=manual. Accessed
17. Ahmed M, McKenzie MO, Puckett S, Hojnacki M, Poliquin L, Lyles DS. 2003. Ability of the Matrix Protein of Vesicular Stomatitis Virus To Suppress Beta Interferon Gene Expression Is Genetically Correlated with the Inhibition of Host RNA and Protein Synthesis, p 4646-57, J Virol, vol 77.
18. Lyles DS. 2000. Cytopathogenesis and Inhibition of Host Gene Expression by RNA Viruses, p 709-24, Microbiol Mol Biol Rev, vol 64.
19. Coulon P, Deutsch V, Lafay F, Martinet-Edelist C, Wyers F, Herman RC, Flamand A. 1990. Genetic evidence for multiple functions of the matrix protein of vesicular stomatitis virus. J Gen Virol 71 (Pt 4):991-6.
20. Tober R, Banki Z, Egerer L, Muik A, Behmüller S, Kreppel F, Greczmiel U, Oxenius A, von Laer D, Kimpel J. 2014. VSV-GP: a Potent Viral Vaccine Vector That Boosts the Immune Response upon Repeated Applications. J Virol 88:4897-907.
21. Geisbert TW, Feldmann H. 2011. Recombinant vesicular stomatitis virus-based vaccines against Ebola and Marburg virus infections. J Infect Dis 204 Suppl 3:S1075-81.
22. Regules JA, Beigel JH, Paolino KM, Voell J, Castellano AR, Hu Z, Muñoz P, Moon JE, Ruck RC, Bennett JW, Twomey PS, Gutiérrez RL, Remich SA, Hack HR, Wisniewski ML, Josleyn MD, Kwilas SA, Van Deusen N, Mbaya OT, Zhou Y, Stanley DA, Jing W, Smith KS, Shi M, Ledgerwood JE, Graham BS, Sullivan NJ, Jagodzinski LL, Peel SA, Alimonti JB, Hooper JW, Silvera PM, Martin BK, Monath TP, Ramsey WJ, Link CJ, Lane HC, Michael NL, Davey RTJ, Thomas SJ. 2015. A Recombinant Vesicular Stomatitis Virus Ebola Vaccine. http://dxdoiorg/101056/NEJMoa1414216.
23. Henao-Restrepo AM, Longini IM, Egger M, Dean NE, Edmunds WJ, Camacho A, Carroll MW, Doumbia M, Draguez B, Duraffour S, Enwere G, Grais R, Gunther S, Hossmann S, Konde MK, Kone S, Kuisma E, Levine MM, Mandal S, Norheim G, Riveros X, Soumah A, Trelle S, Vicari AS, Watson CH, Keita S, Kieny MP, Rottingen JA. 2015. Efficacy and effectiveness of an rVSV-vectored vaccine expressing Ebola surface glycoprotein: interim results from the Guinea ring vaccination cluster-randomised trial. Lancet 386:857-66.
24. Hastie E, Grdzelishvili VZ. 2012. Vesicular stomatitis virus as a flexible platform for oncolytic virotherapy against cancer, p 2529-45, J Gen Virol, vol 93.
25. Liao Y, Smyth GK, Shi W. 2013. The Subread aligner: fast, accurate and scalable read mapping by seed-and-vote. Nucleic Acids Res 41:e108.
26. Ritchie ME, Phipson B, Wu D, Hu Y, Law CW, Shi W, Smyth GK. 2015. limma powers differential expression analyses for RNA-Sequencing and microarray studies. Nucleic Acids Res 43:e47.
27. Pertea M, Kim D, Pertea G, Leek JT, Salzberg SL. 2016. Transcript-level expression analysis of RNA-Seq experiments with HISAT, StringTie, and Ballgown. Nat Protoc 11:1650-67.
28. Kim D, Langmead B, Salzberg SL. 2015. HISAT: a fast spliced aligner with low memory requirements. Nature Methods 12:357.
29. Li H, Handsaker B, Wysoker A, Fennell T, Ruan J, Homer N, Marth G, Abecasis G, Durbin R. 2009. The Sequence Alignment/Map format and SAMtools, p 2078-9, Bioinformatics, vol 25.
30. Li H. 2011. A statistical framework for SNP calling, mutation discovery, association mapping and population genetical parameter estimation from sequencing data, p 2987-93, Bioinformatics, vol 27.

31. Pertea M, Pertea GM, Antonescu CM, Chang TC, Mendell JT, Salzberg SL. 2015. StringTie enables improved reconstruction of a transcriptome from RNA-Seq reads. Nat Biotechnol 33:290-5.
32. Law CW, Alhamdoosh M, Su S, Smyth GK, Ritchie ME. 2016. RNA-Seq analysis is easy as 1-2-3 with limma, Glimma and edgeR. F1000Res 5.
33. Robinson MD, McCarthy DJ, Smyth GK. 2010. edgeR: a Bioconductor package for differential expression analysis of digital gene expression data. Bioinformatics 26:139-40.
34. McCarthy DJ, Chen Y, Smyth GK. 2012. Differential expression analysis of multifactor RNA-Seq experiments with respect to biological variation, p 4288-97, Nucleic Acids Res, vol 40.
35. Luo W, Brouwer C. 2013. Pathview: an R/Bioconductor package for pathway-based data integration and visualization, p 1830-1, Bioinformatics, vol 29.
36. Kandasamy RK, Vladimer GI, Snijder B, Müller AC, Rebsamen M, Bigenzahn JW, Moskovskich A, Sabler M, Stefanovic A, Scorzoni S, Brückner M, Penz T, Cleary C, Kralovics R, Colinge J, Bennett KL, Superti-Furga G. 2016. A time-resolved molecular map of the macrophage response to VSV infection, p 16027-, NPJ Syst Biol Appl, vol 2.
37. Liu J, Qian C, Cao X. 2016. Post-Translational Modification Control of Innate Immunity. Immunity 45:15-30.
38. Blondel D, Harmison GG, Schubert M. 1990. Role of matrix protein in cytopathogenesis of vesicular stomatitis virus. J Virol 64:1716-25.
39. Gaddy DF, Lyles DS. 2005. Vesicular stomatitis viruses expressing wild-type or mutant M proteins activate apoptosis through distinct pathways. J Virol 79:4170-9.
40. Pearce AF, Lyles DS. 2009. Vesicular stomatitis virus induces apoptosis primarily through Bak rather than Bax by inactivating Mcl-1 and Bcl-XL. J Virol 83:9102-12.
41. Diamond MS, Farzan M. 2013. The broad-spectrum antiviral functions of IFIT and IFITM proteins. Nat Rev Immunol 13:46-57.
42. Fleith RC, Mears HV, Emmott E, Graham SC, Mansur DS, Sweeney TR. 2018. IFIT3 and IFIT2/3 promote IFIT1-mediated translation inhibition by enhancing binding to non-self RNA.
43. Fitzgerald KA. 2011. The Interferon Inducible Gene: Viperin, p 131-5, J Interferon Cytokine Res, vol 31.
44. Seo JY, Yaneva R, Cresswell P. 2011. Viperin: a multifunctional, interferon-inducible protein that regulates virus replication. Cell Host Microbe 10:534-9.